AD-A042 759 CALIFORNIA UNIV LOS ANGELES DEPT OF MECHANICS AND ST--ETC F/G 1/3
AN OPTIMALITY CRITERIA APPROACH TO THE MINIMUM WEIGHT DESIGN OF--ETC(U)
MAR 77 M W DOBBS, R B NELSON AF-AFOSR-2640-74
UNCLASSIFIED UCLA-ENG-7731 AFOSR-TR-77-0844 NL

| OF |
ADA042 759

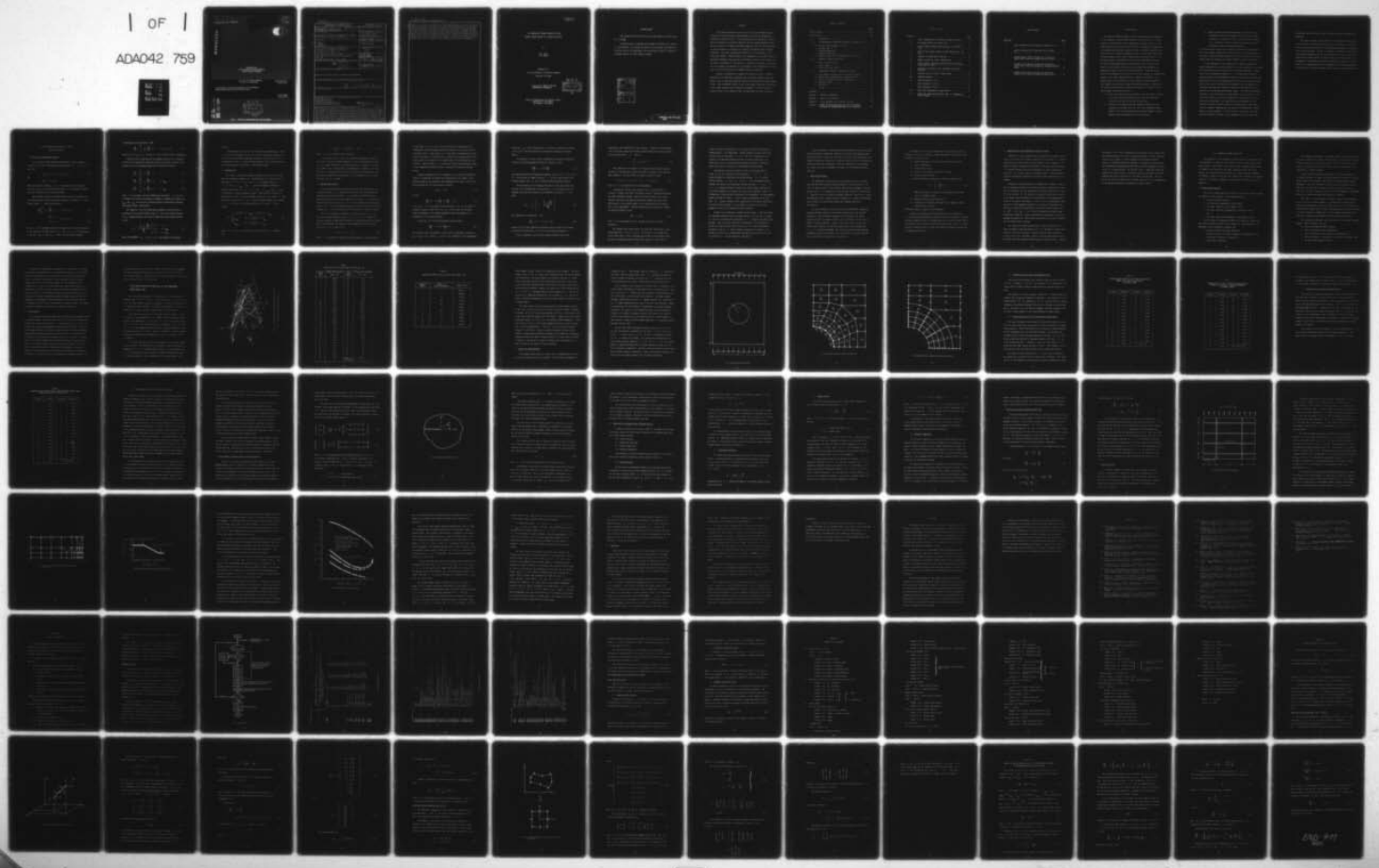

Prepared for the
Air Force Office of Scientific Research
Under Grant No. 74-2640A

UCLA-ENG-7731
MARCH 1977

AN OPTIMALITY CRITERIA APPROACH TO THE MIMIMUM WEIGHT DESIGN OF AIRCRAFT STRUCTURES

M.W. DOBBS
R.B. NELSON

UCLA • SCHOOL OF ENGINEERING AND APPLIED SCIENCE

UNCLASSIFIED

SECURITY CLASSIFICATION OF THIS PAGE *(When Data Entered)*

REPORT DOCUMENTATION PAGE		READ INSTRUCTIONS BEFORE COMPLETING FORM
1. REPORT NUMBER AFOSR-TR-77-0844	2. GOVT ACCESSION NO.	3. RECIPIENT'S CATALOG NUMBER
4. TITLE *(and Subtitle)* AN OPTIMALITY CRITERIA APPROACH TO THE MINIMUM WEIGHT DESIGN OF AIRCRAFT STRUCTURES,		5. TYPE OF REPORT & PERIOD COVERED INTERIM rept. 1 Mar 76 — 1 Mar 77 6. PERFORMING ORG. REPORT NUMBER UCLA-ENG-7731
7. AUTHOR(s) M. W. DOBBS R. B. NELSON		8. CONTRACT OR GRANT NUMBER(s) AF-AFOSR-2640-74 AFOSR 74-2640
9. PERFORMING ORGANIZATION NAME AND ADDRESS UNIVERSITY OF CALIFORNIA - LOS ANGELES MECHANICS AND STRUCTURES DEPARTMENT LOS ANGELS, CA 90024		10. PROGRAM ELEMENT, PROJECT, TASK AREA & WORK UNIT NUMBERS 2307B1 61102F
11. CONTROLLING OFFICE NAME AND ADDRESS AIR FORCE OFFICE OF SCIENTIFIC RESEARCH/NA BLDG 410 BOLLING AIR FORCE BASE, D C 20332		12. REPORT DATE March 1977 13. NUMBER OF PAGES 93
14. MONITORING AGENCY NAME & ADDRESS *(if different from Controlling Office)* 16 2307 17 B1		15. SECURITY CLASS. *(of this report)* UNCLASSIFIED 15a. DECLASSIFICATION/DOWNGRADING SCHEDULE

16. DISTRIBUTION STATEMENT *(of this Report)*

Approved for public release; distribution unlimited.

17. DISTRIBUTION STATEMENT *(of the abstract entered in Block 20, if different from Report)*

14 UCLA-ENG-7731

18. SUPPLEMENTARY NOTES

19. KEY WORDS *(Continue on reverse side if necessary and identify by block number)*

STRUCTURAL DESIGN
OPTIMALITY CRITERIA
KUHN-TUCKER OPTIMALITY TEST
FRACTURE MECHANICS CONSTRAINT

409458

20. ABSTRACT *(Continue on reverse side if necessary and identify by block number)*

The research presented in this report is both a continuation and an extension of the optimality criteria approach to structural optimization reported in AFOSR-TR-75-1431. In the present study the optimality criteria method is extended to provide a capability for the automated minimum weight design of elastic, redundant structures composed of one-and two-dimensional structural elements and subjected to multiple, independent static loading conditions. The design variables are taken to be the thicknesses of the structural elements. These variables are constrained to be between specified maximum and minimum values, as are the

DD FORM

internal stresses in each element and the nodal displacements of the structure. Results are presented to indicate both the excellent performance of the optimality criteria method and the wide range of structures which can be designed using the algorithm. Finally, the algorithm is extended to include the new (to automated design) and very important requirement that structural integrity under the applied loads be maintained given the presence of existing structural fatigue cracks. This requirement, which is cast in an energy format and incorporated in the design algorithm as an inequality constraint, is shown to have a dominant effect in the design of safe, minimum weight aircraft structures.

UCLA-ENG-7731
MARCH 1977

AN OPTIMALITY CRITERIA APPROACH TO THE MINIMUM WEIGHT DESIGN OF AIRCRAFT STRUCTURES

by

M.W. Dobbs
R.B. Nelson

Prepared for

Air Force Office of Scientific Research

Grant No. 74-2640A

**Approved for public release;
distribution unlimited.**

School of Engineering and Applied Science
University of California
Los Angeles, California

ACKNOWLEDGMENT

The research described in this report was supported by AFOSR Grant No. 74-2640A.

The authors wish to express their thanks to Professor L.A. Schmit, Jr. and Professor L.P. Felton, who serve as Co-Principal Investigators on the grant, and Mr. William Walker, the AFOSR Grant Officer and cognizant technical monitor for this research program.

ABSTRACT

The research presented in this report is both a continuation and an extension of the optimality criteria approach to structural optimization reported in AFOSR-TR-75-1431. In the present study the optimality criteria method is extended to provide a capability for the automated minimum weight design of elastic, redundant structures composed of one- and two-dimensional structural elements and subjected to multiple, independent static loading conditions. The design variables are taken to be the thicknesses of the structural elements. These variables are constrained to be between specified maximum and minimum values, as are the internal stresses in each element and the nodal displacements of the structure. Results are presented to indicate both the excellent performance of the optimality criteria method and the wide range of structures which can be designed using the algorithm.

Finally, the algorithm is extended to include the new (to automated design) and very important requirement that structural integrity under the applied loads be maintained given the presence of existing structural fatigue cracks. This requirement, which is cast in an energy format and incorporated in the design algorithm as an inequality constraint, is shown to have a dominant effect in the design of safe, minimum weight aircraft structures.

TABLE OF CONTENTS

LIST OF FIGURES

LIST OF TABLES

I. INTRODUCTION

The research presented herein is both a continuation and an extension of the optimality criteria method developed on AFOSR Grant No. 74-2640A, reported in AFOSR-TR-75-1431 and subsequently published in Ref. 1. This research activity has been concerned with the development of a capability for automated minimum weight design of elastic, redundant aircraft structures subjected to multiple independent static loading conditions and constrained against several types of inadmissable structural behavior. The activity reported in AFOSR-TR-75-1431 was quite fundamental in nature; the basic redesign algorithm was developed and tested on elastic truss-type structures subject to only stress constraints and constraints on maximum and minimum values of the design variables. While the results were very encouraging for this rather restrictive problem, the computational aspects of the design algorithm were not completely understood. In a broader sense, the applicability of the optimality criteria approach to more complex (and practical) design problems was untested. Therefore, in the research activity which followed that presented in AFOSR-TR-75-1431, three primary objectives have been to:

(1) Extend and refine the basic optimality criteria method to improve its already efficient performance and reduce the experience required by the user to exercise the algorithm.

(2) Increase the structural modeling capability contained in the algorithm to the point where two- and three-dimensional assemblages of one- and two-dimensional structural elements could be designed using the optimality criteria algorithm.

(3) Extend the types of design constraints to include stress, displacement, minimum and maximum constraints on the design variables, and constraints based on gross structural behavior, i.e., constraints included in other existing algorithms for the design of elastic redundant structures.

To a certain extent, these three research objectives were interrelated since, for example, algorithmic performance could be adequately measured only after developing design experience with structures more complex than trusses which are subjected to several different types of constraints.

In the development of the capability for treating constraints against inadmissible structural behavior, the usual constraints on stresses and displacements were incorporated into the design algorithm. However, since a rather substantial literature [2 - 5] demonstrates the ease with which optimality criteria methods can deal with constraints on gross structural behavior (e.g., on minimum natural frequencies or elastic buckling loads) a new type of constraint was incorporated into the algorithm; a constraint requiring the structure to maintain its integrity given the presence of existing structural fatigue cracks. This fracture mechanics constraint, which can be cast in a form based on energy concepts for the structure, provides a test of the capability of the algorithm to treat energy-type constraints. More importantly, the development of this fracture constraint provides a means for establishing the effect that fracture mechanics considerations can play in determining safe, minimum weight structural designs. As will be shown in this Report, this new fracture mechanics constraint is very important and in fact may govern

the minimum weight structural design of typical aircraft structural sub-assemblies.

This Report contains a brief review of the mathematical foundations of the optimality criteria method utilized in this research in Section II, as well as a general discussion of the computational features incorporated in the design algorithm. Section III contains a description of the structural modeling capability of the present algorithm and also a review of its computational characteristics for several well known test problems. The development of the fracture constraint is described in detail in Section IV as well as its implementation in the optimality criteria design algorithm. A discussion of the results obtained in this research is given in Section V.

II. THE MATHEMATICAL OPTIMALITY CRITERIA AND REDESIGN RULE

A. Review of the Optimality Criteria

The structural weight minimization problem is stated formally as follows: find a set of independent design variables D_j, $j = 1,2,\ldots,N$, such that

$$g_k(D_j) \leq 0, \qquad k = 1,2,\ldots,M \tag{1}$$

and

$$W(D_j) \longrightarrow \min$$

where the objective function $W(D_j)$ is the weight and the constraint functions $g_k(D_j)$ are behavioral constraints on the structural response and side constraints on the design variables.

The necessary criteria for optimum design, which are the basis for the present method, are the Kuhn-Tucker necessary conditions [6]. For an optimum Design D_j these conditions are,

$$\frac{\partial W}{\partial D_j} + \sum_{k}^{M} \lambda_k \frac{\partial g_k}{\partial D_j} = 0, \qquad j = 1,2,\ldots,N \tag{3}$$

$$\lambda_k g_k = 0, \qquad k = 1,2,\ldots,M$$

$$\lambda_k \geq 0, \tag{4}$$

where λ_k is the Lagrange multiplier associated with the k-th constraint. If the constraint is noncritical, $g_k < 0$ and $\lambda_k = 0$; if the constraint is critical, $g_k = 0$ and $\lambda_k \geq 0$. Thus, the Kuhn-Tucker necessary

conditions may be simplified to read

$$\frac{\partial W}{\partial D_j} + \sum_{k}^{\bar{K}} \lambda_k \frac{\partial g_k}{\partial D_j} = 0 \qquad j = 1,2,\ldots,N \tag{5}$$

where $g_k = 0$ and $\lambda_k \geq 0$ for all $\bar{K}$ $(\leq M)$ active critical constraints.

The active side constraints on the design variables can be separated from the active behavioral constraints and the Kuhn-Tucker necessary conditions for a local optimum design can be rewritten as follows:

$$\frac{\partial W}{\partial D_j} + \sum_{k}^{K} \lambda_k \frac{\partial g_k}{\partial D_j} = 0 \qquad j \quad J \tag{6}$$

$$\frac{\partial W}{\partial D_j} + \sum_{k}^{K} \lambda_k \frac{\partial g_k}{\partial D_j} \leq 0 \qquad j \in J_{max} \tag{7}$$

$$\frac{\partial W}{\partial D_j} + \sum_{k}^{K} \lambda_k \frac{\partial g_k}{\partial D_j} \geq 0 \qquad j \in J_{min} \tag{8}$$

where K is the number of active behavioral constraints, J is the set of design variables not constrained by minimum or maximum side values, and J_{max} and J_{min} are the sets of design variables constrained by maximum and minimum values, respectively.

The separated form of the Kuhn-Tucker necessary conditions can be rewritten by dividing both sides of Eqs. (6) - (8) by the weight gradient $\partial W/\partial D_j$ (assumed positive, the case for most structural design problems) to give

$$I_j = \frac{-\sum_{k}^{K} \lambda_k \frac{\partial g_k}{\partial D_j}}{\frac{\partial W}{\partial D_j}} \begin{cases} = 1, & j \in J \\ \geq 1, & j \in J_{max} \\ \leq 1, & j \in J_{min} \end{cases} \tag{9}$$

where the parameters I_j, $j = 1,2,\ldots,N$, are defined as the design

factors.

The relations in Eq. (9) are the criteria for minimum weight. That is, if for a given design, the set of K active behavioral constraints is such that the corresponding Lagrange multipliers are positive and Eq. (9) is satisfied for all j, then the design satisfies the Kuhn-Tucker necessary conditions and is therefore a local optimum design.

B. Redesign Rule

The form of Kuhn-Tucker necessary conditions given by Eq. (9) suggests an associated redesign rule. Qualitatively, the criteria of Eq. (9) imply that: (1) if $I_j \equiv 1.0$, then D_j is optimally sized; (2) if $I_j > 1.0$ and $D_j < D_{j_{max}}$, then D_j must be increased to obtain an improved design; and (3) if $I_j < 1.0$ and $D_j > D_{j_{min}}$, then D_j must be decreased to obtain an improved design. Therefore, the iterative redesign rule is taken to be the following: given the α-th design D_k^{α} with associated design factors $I_j(D_k^{\alpha})$, then the design variables at iteration $(\alpha + 1)$ are related to the design variables at iteration α by the relation

$$D_j^{\alpha+1} = \begin{cases} f[I_j(D_k^{\alpha})]D_j^{\alpha} & \text{if } D_{j_{min}} < f[I_j(D_k^{\alpha})]D_j^{\alpha} < D_{j_{max}} \\ D_{j_{max}} & \text{if } f[I_j(D_k^{\alpha})]D_j^{\alpha} \geq D_{j_{max}} \\ D_{j_{min}} & \text{if } f[I_j(D_k^{\alpha})]D_j^{\alpha} \leq D_{j_{min}} \end{cases} \tag{10}$$

where $f(1.0) = 1.0$. In the present study the function f is taken to be

$$f[I_j(D_k^{\alpha})] = [I_j(D_k^{\alpha})]^{1/2} = I_j^{1/2} \tag{11}$$

where I_j is the design factor at iteration α.

This redesign rule is exact for statically determinate structures with weight functions linearly dependent on the design variables and subject to a single frequency or buckling constraint, or subject to a single load condition and a single stress or displacement constraint. The redesign rule is approximate for the design of statically indeterminate structures and/or multiple load conditions. It is emphasized that the design objective, Eq. (9), is exact.

C. Computational Aspects

The following sequence of operations defines each iteration of the redesign procedure: (1) identify the active and near-active behavioral constraints and side constraints; (2) calculate the gradients and Lagrange multipliers of the active behavioral constraints; (3) evaluate the design factors defined by Eq. (9); (4) either terminate the redesign procedure if Eq. (9) is identically satisfied or resize the structure using the redesign rule. A brief description of each operation is described below.

The k-th behavioral constraint is strictly active if $g_k \equiv 0.0$, or if the so-called response ratio, $R_k = g_k + 1.0 \equiv 1.0$. However, for numerical purposes a behavioral constraint is identified as active (or near active) and governing the redesign if its response ratio is arbitrarily close to one (1.0), that is, if

$$1.0 - \beta \leq R_k \leq 1.0 \tag{12}$$

where β is a preselected constraint buffer parameter, usually contained

in the range $0.04 \leq \beta \leq 0.10$. The identification of near-active constraints and the final weight obtained are sensitive to the value of the constraint buffer. Large values of β allow early identification of near-active constraints but usually result in heavy final designs because of the large spread in the values of the response ratios of the near-active constraints. Smaller values of β usually give lighter final designs because of the comparitively smaller spread in near-active constraint response ratios.

Analytic expressions for the components of the constraint gradients (that is, derivatives of stresses and displacements with respect to the design variables) are obtained by differentiating both sides of the stiffness relations for the linear elastic structure

$$[K]\{u\} = \{F\} \tag{13}$$

to give

$$\frac{\partial[K]}{\partial D_j}\{u\} + [K]\frac{\partial\{u\}}{\partial D_j} = \frac{\partial\{F\}}{\partial D_j} = \{0\} \quad . \tag{14}$$

In Eq. (13), $[K]$ is the system stiffness matrix, $\{F\}$ is the vector of equivalent applied nodal forces and $\{u\}$ is the vector of developed nodal displacements. The applied mechanical loads are assumed to be independent of the design variables.

Solving Eq. (14) for the displacement gradient gives

$$\frac{\partial\{u\}}{\partial D_j} = -[K]^{-1}\frac{\partial[K]}{\partial D_j}\{u\} \quad . \tag{15}$$

For a given design, the gradients of the active displacement constraints, $g_k = (u_i/u_\ell) - 1.0$, where u_i is the i-th component of the displacement

vector and u_ℓ is the limiting value, is obtained by reducing the product $(\partial[K]/\partial D_j)\{u\}$ and back substituting through the decomposed stiffness matrix.

The gradient of active stress constraints is obtained by differentiating the stress-displacement relation for a member to give

$$\frac{\partial\{\sigma\}}{\partial D_j} = [D][B]\frac{\partial\{u\}}{\partial D_j} \tag{16}$$

and substituting for the displacement gradient from Eq. (15). In Eq. (16), $\{\sigma\}$ is the vector of element stresses, $[D]$ is the linear elastic constitutive matrix and $[B]$ is the linear strain-displacement matrix.

The calculation of the Lagrange multipliers of the near-active constraints can be accomplished in several ways. In the present study, the Lagrange multipliers are evaluated by minimizing the function $\mathcal{J} = \mathcal{J}(\lambda)$ where

$$\mathcal{J}(\lambda) = \sum_j^J \left[1 + \frac{\sum_k^K \lambda_k \frac{\partial g_k}{\partial D_j}}{\frac{\partial W}{\partial D_j}} \right]^2 . \tag{17}$$

The conditions for minimizing $\mathcal{J}$ are

$$\frac{\partial \mathcal{J}}{\partial \lambda_k} = 0, \quad k = 1,2,\ldots,K \tag{18}$$

giving a set of linear algebraic equations, equal in number to the number of near-active constraints, to solve for the Lagrange multipliers.

Since, in general, there are more design variables than active

constraints, the minimization of the function Φ amounts to the minimization of the mean square error between current values of the design factors and the optimum value 1.0 that is,

$$\Phi = \sum_{j}^{J} (I_j - 1.0)^2 \quad . \tag{19}$$

Move limits must be imposed on the design factors before resizing, because the redesign rule is valid only near the optimum and is approximate elsewhere. The move limits are taken as uniform so that

$$1.0 - |\Delta| \leq I_j \leq 1.0 + |\Delta|, \qquad j = 1,2,\ldots,N \tag{20}$$

where $|\Delta|$ is a preselected move limit parameter.

Resizing the structure may cause the set of current active restraints to change (constraint switching); excessive constraint switching may cause infeasible designs. Small move limits minimize this effect. However, constraint switching and infeasible designs may still occur, particularly in the initial stages of the redesign where the resizing rule is most approximate. Feasible designs are then obtained by scaling the design variables so that

$$\bar{D}_j^{\alpha+1} = \bar{R}\, D_j^{\alpha+1} \tag{21}$$

where $\bar{R}$ is the response ratio of the most active (and violated) constraint.

For problems with stress limits only the move limits must be relatively small with $0.04 \leq |\Delta| \leq 0.08$. (In addition, for problems with stress limits only, a fully stressing move is made on those design variables with corresponding design factors less than zero. This move is

useful in quickly identifying the set of design variables constrained by minimum values.) For displacement - limited problems the move limits may be greater and are typically $|\Delta| = 0.25$. The set of near-active constraints in displacement-limited problems is usually smaller and more stable than the set in stress-limited problems; therefore, relatively larger move limits are possible in displacement-limited design.

Computational experience indicates that the following default values for the two preselected design parameters β and $|\Delta|$ are usually adequate for obtaining near optimum designs: (1) for stress-limited problems, $\beta = 0.08$, $|\Delta| = 0.08$; (2) for displacement-limited problems (and stress and displacement limited problems), $\beta = 0.10$, $|\Delta| = 0.25$. It is usually possible to improve the final designs obtained with the default parameters by reducing the value of the constraint buffer β, although more iterations may be necessary for convergence. For displacement-limited problems the buffer β can be chosen independently of the move limit $|\Delta|$. However, because of the sensitivity of the stress constraints in stress-limited problems, it is necessary to reduce the move limit parameter as well as the constraint buffer parameter.

Finally, it is necessary to modify the functional $\mathcal{J}$ and recalculate the Lagrange multipliers and the design factors if, in the trial resizing, (1) new side constraints are identified, or (2) negative multipliers are obtained. When a new side constraint is identified, it is necessary to delete the design variable from the sum in Eq. (17) over the variables contained in the set J. When a negative multiplier is obtained, it is necessary to delete the corresponding constraint from the sum in Eq. (17) over the set of K active behavioral constraints.

Both the deletion of design variables associated with side constraints and the deletion of behavioral constraints associated with negative multipliers may require, within each redesign cycle, one or more iterations (one complete solution per iteration) to obtain a stable list of side constraints and active behavioral constraints. When the constraint lists stabilize, the resized structure is analyzed and scaled and the redesign procedure reentered.

D. Algorithm Efficiency

The optimality criteria method of the present study is in general less efficient than previous physical optimality criteria methods. However, the present method is more general than previous optimality criteria methods since: (1) convergence to local optimum designs is obtained; and (2) special forms for different behavioral constraint types are not needed. The generality of the present method is obtained at a greater computational cost, primarily for constraint gradient and Lagrange multiplier calculations.

The present method is more efficient than mathematical programming methods, primarily because of the relative simplicity of the resizing calculation. The efficiency advantage is most prevalent for design problems in which the number of final active constraints is less than the number of design variables. However, the results for the 63-bar truss stress-limited problem [7] show the present method with a significant (2 to 1) efficiency advantage over the latest generation mathematical programming methods for problems with a large number of design variables and a large number of final active constraints.

The computer code for the present method incorporates a number of features to reduce both computer storage requirements and execution time. Briefly, these features are:

(1) dynamic allocation of all arrays in terms of the relevant control parameters;

(2) overwriting of arrays;

(3) storage of only non-zero degrees of freedom;

(4) design variable linking;

(5) system stiffness calculation by stiffness gradients with

$$[K] = \sum_{j}^{N} \frac{\partial [K]}{\partial D_j} [D_j] \qquad (22)$$

where the stiffness gradients are calculated only once and stored in compacted form;

(6) analytic gradient calculations; and

(7) elimination of dependent gradients (due to symmetry related design variable linking).

Additional details are given in the Appendix A.

Further and significant efficiency gains could be obtained by: (1) incorporating approximation concepts to reduce the number of complete structural analyses (that is, decomposition of the system stiffness matrix and reduction and back substitution of the load vectors); and (2) using iterative solution methods to reduce the number of complete solutions for the Lagrange multipliers.

E. Comparison with Other Optimality Criteria Methods

Optimality criteria methods using the Kuhn-Tucker necessary conditions as the criteria for optimum design have been proposed [4]. However, the associated redesign rules in these methods do not, in general, converge to designs satisfying the Kuhn-Tucker necessary conditions because: (1) elements governed by stress constraints are resized using stress ratio; and (2) in most cases the "envelope method" is used wherein resizing is accomplished considering the most critical constraint for each element.

Optimality criteria methods with redesign rules capable of converging to designs satisfying the Kuhn-Tucker necessary conditions were proposed by Kiusalaas [3] (and implemented for multiple constraints by Rizzi [8]) and by Terai [9]. The method of Kiusalaas differs from the method of the present study primarily in the calculation of the Lagrange multipliers of the active constraints. In Ref. 8 a set of simultaneous linear equations for the Lagrange multipliers is obtained by requiring strict activity of constraints identified as near-active during resizing; that is, $g_k^{\alpha+1} = g_k^{\alpha} + \Delta g_k \equiv 0.0$. The set of equations is solved using Gauss-Seidel iteration. Inactive constraints corresponding to negative Lagrange multipliers are deleted when encountered and the side constraint list is updated before resizing.

The results for design problems with a small and stable list of final constraints shows the method of Ref. 8 to converge to designs satisfying the Kuhn-Tucker necessary conditions with all final constraints strictly active (and, therefore, capable of giving final designs lighter in weight than final designs obtained using the present method). However,

the method of Ref. 8 has no advantage over the method of the present study for problems having a set of active constraints which is neither small nor stable as, for example, in large primarily stress-limited problems. Indeed, the potential efficiency advantage of optimality criteria methods over mathematical programming methods may be lost when applying the method of Ref. 8 to large problems. The results of Ref. 8 imply that infeasible designs with a large number of active and violated constraints are needed from the beginning to properly sort the final constraint set. This requires the solution of large sets of linear equations for the determination of the Lagrange multipliers throughout the design process.

III. EXTENDED MODELING CAPABILITY

The generality of the optimality criteria method of the present study is demonstrated by results for the design of trusses, plates and stiffened plate systems. These results were obtained using a computer program coded in FORTRAN IV for use on the UCLA Campus Computing Network IBM 360/91 system. All calculations were performed in a single precision arithmetic; the FORTRAN G compiler option was used, unless noted otherwise. The program structure is described in Appendix A and required data cards are listed in Appendix B.

A. Finite Element Library

Five finite element types are included in the present computer program for numerical stress analysis. These element types are:

1. the two-node truss element;
2. the three-node subparametric truss element;
3. the planar constant strain triangle (CST);
4. the planar four-node isoparametric quadrilateral (QUAD4); and
5. the planar eight-node isoparametric quadrilateral (QUAD8).

The more complex isoparametric elements are preferred in nearly all cases over the simple constant strain triangle for planar analysis. The advantages of the isoparametric elements are:

1. improved structural modeling capability;
2. improved accuracy over simple triangles and rectangles for the same number of degrees of freedom; and
3. reduced data preparation.

The primary disadvantage of the complex elements is the extra effort required to generate the element stiffness matrix. However, since element stiffness matrices are calculated only once (to form the stiffness gradients), the additional cost of the initial stiffness calculation is not significant in a design program.

Element stiffness matrices are obtained by numerical integration. The complex elements are mapped into simple shapes in a natural coordinate system in which the stiffness coefficients are evaluated using Gaussian quadrature. (Two-point quadrature is used for the three-node truss element, two- and three-point formulas are used for the QUAD4, and two-, three- and four-point formulas are used for the QUAD8 element.) Additional details on stiffness generation are included in Appendix C.

Note that it is not necessary to retain a constant strain triangle (as is done in the present program). A straight-sided triangle may be formed by collapsing one side and two nodes of the QUAD4 to a single node; a curved-sided triangle may be formed by collapsing one side and three nodes of a QUAD8 element to a single node. The CST element is presently used only in the transition zone between fine and coarse element grids.

Four behavioral constraint types are included in the present computer program. These constraint types are:

1. limits on allowable element stresses;
2. limits on allowable nodal displacements;
3. limits on allowable relative nodal displacements; and
4. fracture mechanics constraints, i.e., limits on developed opening mode stress intensity factors.

Application of mathematical optimality criteria methods to buckling and frequency constraints has been demonstrated by Terai [9] (with special forms of the redesign rule for problems with only one active constraint type). Application to aeroelastic flutter constraints has been demonstrated by Rizzi [8] so that these results are not duplicated in the present study. Rather, a new constraint type, against fast fracture, is considered. The need to include fracture constraints in analysis and design is evidenced by the increasing volume of literature on the subject in a number of structural engineering problems, ranging from nuclear reactor components to lightweight aircraft components. Little work has been done to rationally include fracture constraints in automated design. This important design consideration is described in detail in Section IV.

B. Truss Results

Both two- and three-dimensional truss problems were investigated using the present methods. Results for the 3, 10, 25, 63 and 72 bar trusses with stress limits only are given in Ref. 7. Results for the 10, 25 and 63 bar trusses with stress and displacement limits are given in Ref. 1. These results compare favorable with previous results obtained by both mathematical programming and physical optimality criteria methods. The present method is effective in generating near optimum designs and is capable of converging to true optimum designs when the physical optimality criteria methods cannot. The present method is also very efficient compared to the most recent design methods based on mathematical programming. The number of complete structural analyses needed in the present method are essentially the same as the number needed in the mathematical programming methods, but

the redesign procedure is much less costly. This efficiency is retained for large problems as illustrated by the results for the 63-bar truss wing carry through box. These results are reviewed because of the importance of this problem in the literature.

63-bar truss wing carry through box, two load conditions, stress limits only.

The structural configuration is shown in Fig. 1. The material is titanium with $E = 16.0 \times 10^6$ psi., $\rho = 0.16$ pci., and $\sigma_y = \pm 100.0 \times 10^3$ psi. No design variable linking is specified; therefore, this problem has 63 independent design variables. A minimum area constraint = 0.01 $in.^2$ is imposed on the design variables; maximum limits are not imposed.

The problem was initiated from a uniform starting design. A weight of 5145 lbs. was obtained after 15 analyses using the stress-limited default design parameters $\beta = 0.08$ and $|\Delta| = 0.08$. An improved result with $W = 5026$ lbs. was obtained after 12 analyses with $\beta = 0.06$ and $|\Delta| = 0.05$. These results, detailed in Table 1, compare favorably with the stress ratio design of 5034 lbs. after 50 analyses [4] and the design obtained using mathematical programming [10] with $W = 4977$ lbs. after 14 analyses.

It is clear from Table 2 that the convergence of the present method is not monotonic. The fluctuation in the number of active constraints is primarily due to: (1) the approximations inherent in the redesign rule; (2) the sensitivity of member stresses to changes in member areas; and (3) the large number of active constraints in the final design. The

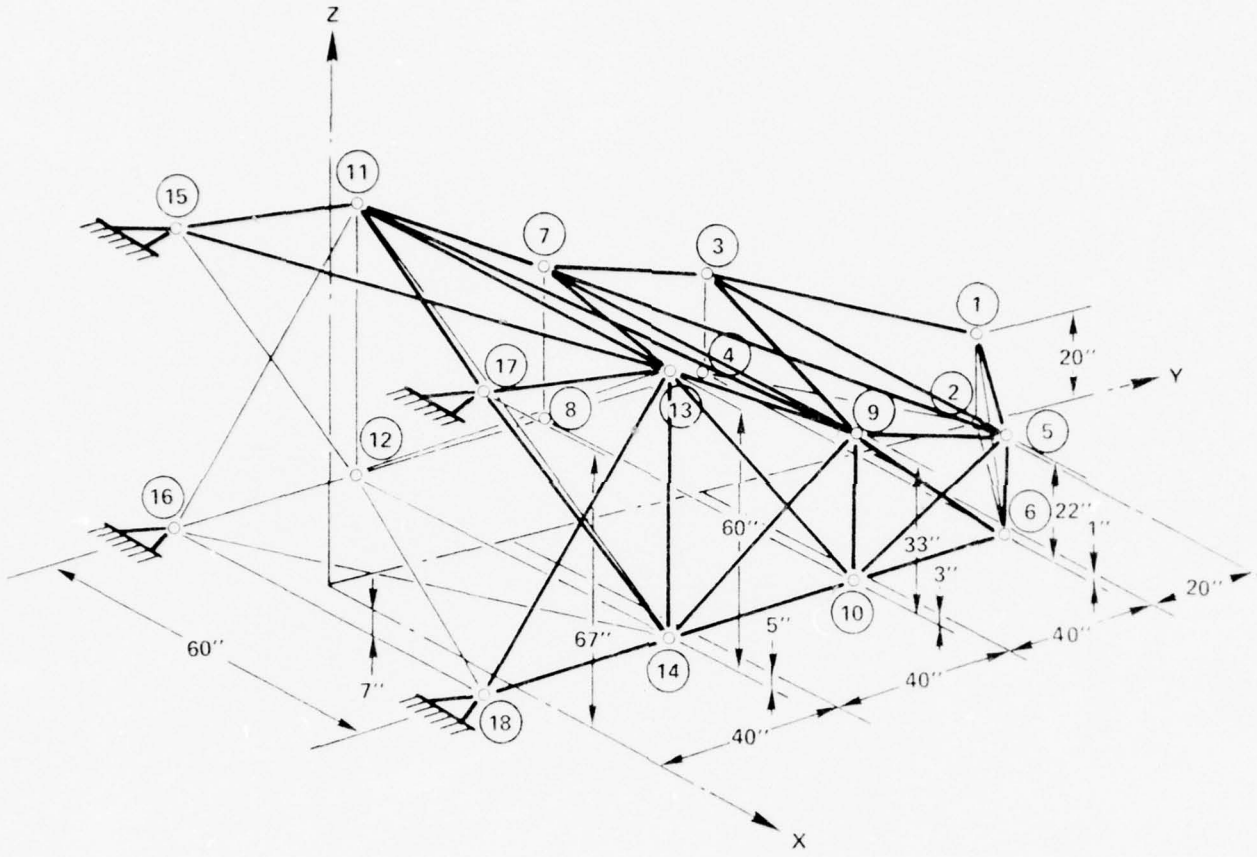

Note: For the sake of clarity, not all elements are drawn in this figure.

Fig. 1. Truss Idealization of Wing Carry Through Structure

TABLE 1

FINAL DESIGNS FOR 63-BAR WING CARRY THROUGH BOX

Truss Member No.	Final Cross Section Areas (in^2)	Truss Member No.	Final Cross Section Areas (in^2)
1	38.36	33	5.26
2	36.53	34	5.85
3	52.66	35	5.26
4	54.53	36	3.27
5	25.24	37	3.36
6	28.55	38	3.33
7	17.87	39	3.44
8	20.73	40	5.31
9	25.14	41	5.19
10	27.12	42	16.03
11	7.59	43	18.42
12	9.16	44	11.69
13	24.08	45	14.09
14	20.53	46	11.82
15	4.16	47	6.45
16	2.62	48	11.90
17	37.39	49	13.85
18	37.58	50	7.47
19	0.01	51	7.65
20	0.01	52	5.35
21	0.38	53	.20
22	0.18	54	3.56
23	0.01	55	9.45
24	1.11	56	4.30
25	0.34	57	.47
26	2.93	58	.01
27	1.08	59	.01
28	4.72	60	.01
29	0.85	61	.01
30	3.12	62	.01
31	3.36	63	.01
32	5.57	Weight (lbs)	5026.4
		Iterations	11

TABLE 2

ITERATION HISTORY FOR 63-BAR WING CARRY THROUGH BOX

Analysis Number	Number of Active Constraints	Weight (lbs)
1	2	30214.2
2	6	6387.0
3	9	5795.0
4	18	5428.3
5	11	5501.3
6	2	5667.0
7	33	5272.8
8	27	5286.9
9	6	5462.2
10	1	5747.3
11	44	5026.4

final designs in Refs. 4 and 10 are essentially fully stressed. The final design in Ref. 10 has 58 active stress constraints and five active minimum area constraints. The final design of the present study has 44 active stress constraints and nine active minimum area constraints; this design is not completely converged since the Kuhn-Tucker necessary conditions are not identically satisfied. However, the square root of the design factors of 42 of the 54 nonminimum area bars are converged to $\pm$ 5 percent of unity and the remaining design factors are converged to $\pm$ 10 percent of unity. Continued redesign does not lead to large changes in variable sizes or final weight.

The final results for this problem using the present method required 18 CPU sec. for execution on the IBM 360/91, using the FORTRAN H compiler. The method of Ref. 10 required approximately 48 CPU sec. of execution time on the same IBM 360/91 computer and the FORTRAN H compiler for a one percent overweight design (W = 5045 lbs.), using default design parameters. Subsequent results in Ref. 10 with design parameters selected to speed convergence required approximately 36 CPU sec. for a one percent overweight design (W = 5025 lbs.). Thus, the present optimality criteria method retains a computational efficiency advantage over mathematical programming methods even when the number of design variables is larger than the number of degrees of freedom and the number of final active constraints is not small compared to the number of design variables.

C. Center Hole Plate Results

The minimum weight design of a center hole rectangular plate subject to a uniform tensile stress is considered. The structural configuration

is shown in Fig. 2. Three design cases are considered: (1) unreinforced hole with stress and minimum side limits; (2) unreinforced hole with stress, minimum and maximum side limits; and (3) reinforced hole with stress and minimum side limits. Plane stress conditions are assumed.

Due to symmetry, only a quarter of the plate need be considered. The finite element idealization of the quarter plate is shown in Fig. 3. The skin is modeled by 29 planar four-node isoparametric quadrilaterals and the reinforcement by five two-node truss elements. No design variable linking is imposed and there are 34 design variables, the thicknesses of the 29 planar elements and the areas of the five truss elements. Numerical integration for the stiffness is accomplished by two-point Gaussian quadrature. The largest of the integration point Von Mises equivalent stresses of an element is assumed to govern the design of the element. Initial stress analysis of the unreinforced plate is checked against results obtained using the finite element model with 18 eight-node quadrilaterial elements (Fig. 4).

For all three cases, the applied tensile stress is $\sigma_a = 21{,}704.4$ psi. and the material is aluminum 7075 T6 (with $E = 10.8 \times 10^6$ psi., $\nu = 0.333$, $\rho = 0.1$ pci. and $\sigma_y = \pm 80.0 \times 10^3$ psi.). A minimum side limit = 0.01 in. is imposed in all cases. All results were obtained using the stress limited default parameters $\beta = 0.08$ and $|\Delta| = 0.08$. All results appear to compare favorably with the design presented by Pope [11], but only a qualitative comparison is possible since Pope does not provide loading or material property information. Pope's study also was slightly different since his design variables were the nodal thicknesses.

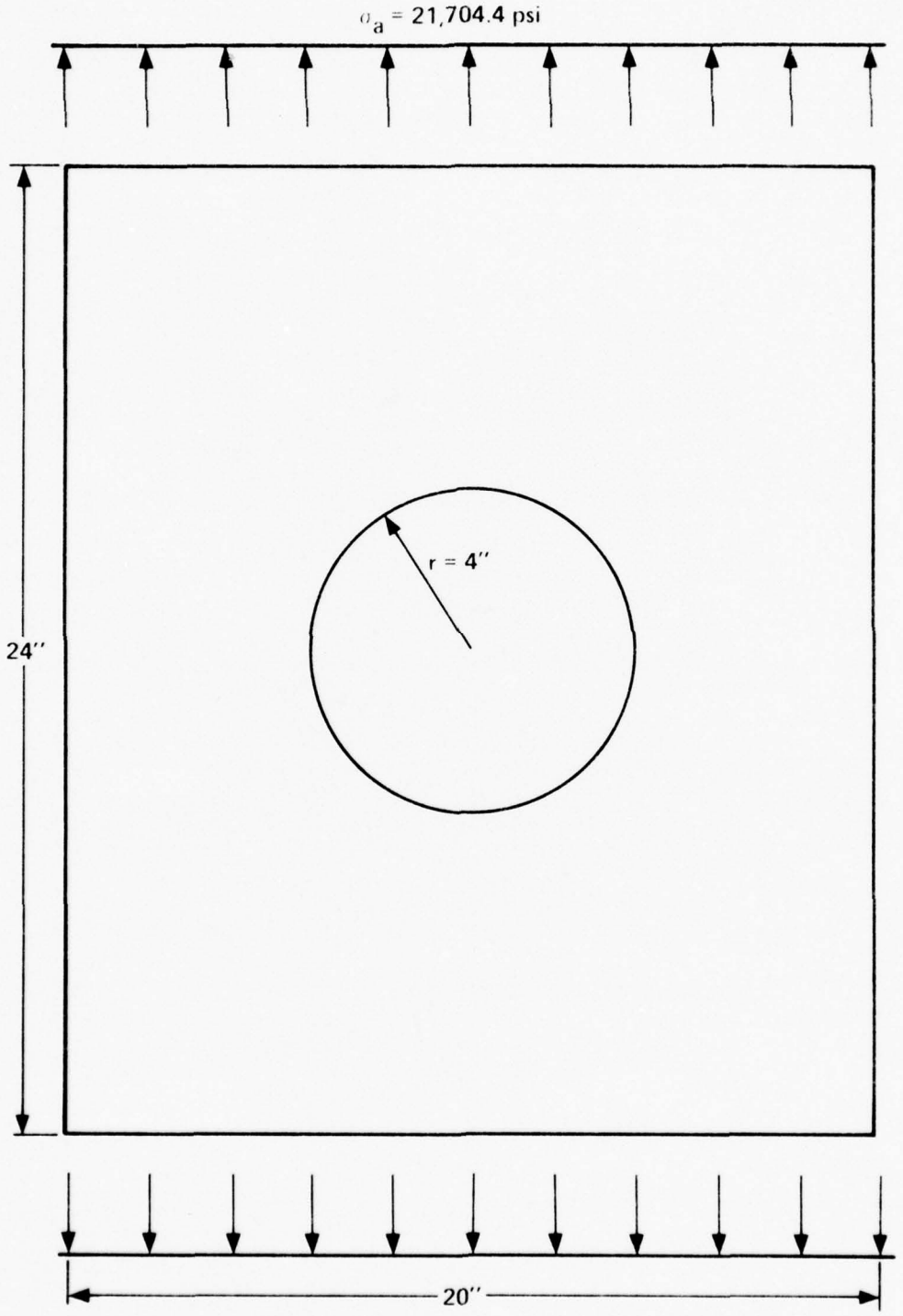

Fig. 2. Rectangular Plate with Center Hole

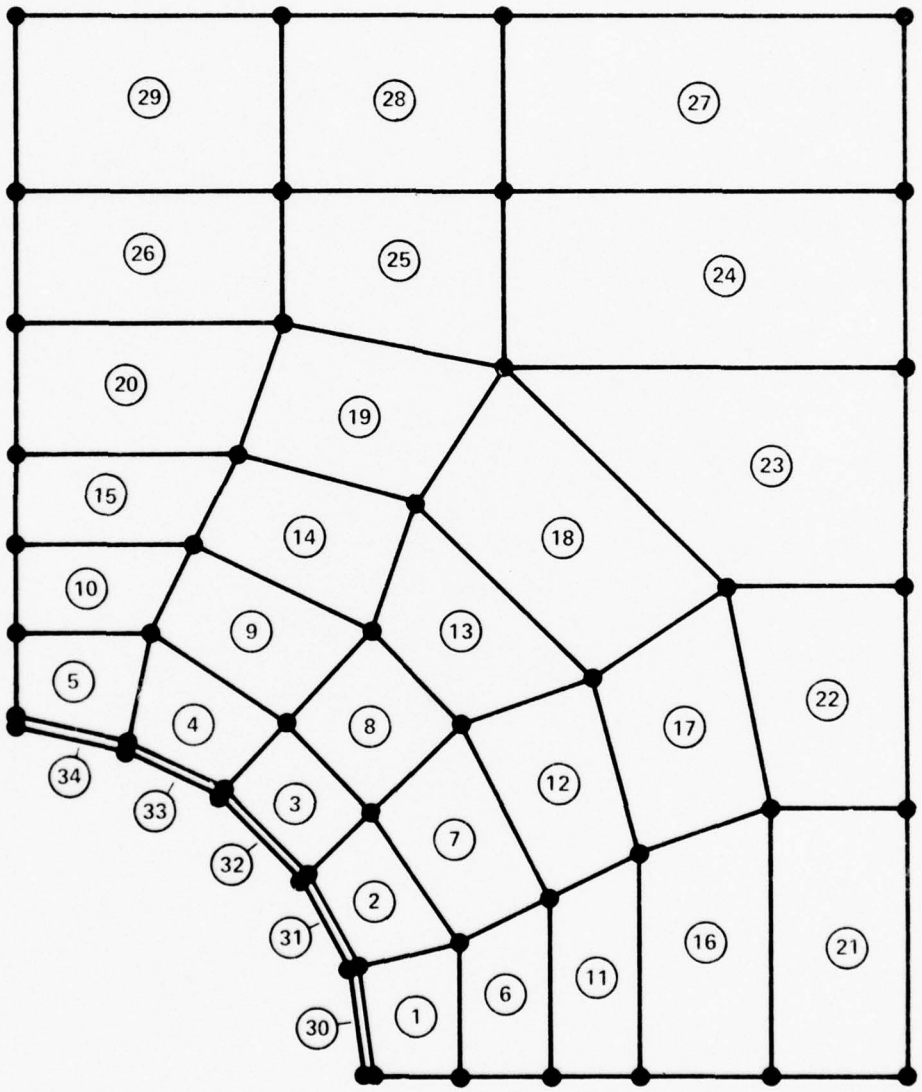

Fig. 3. Finite Element Idealization of Quarter of Stiffened Plate

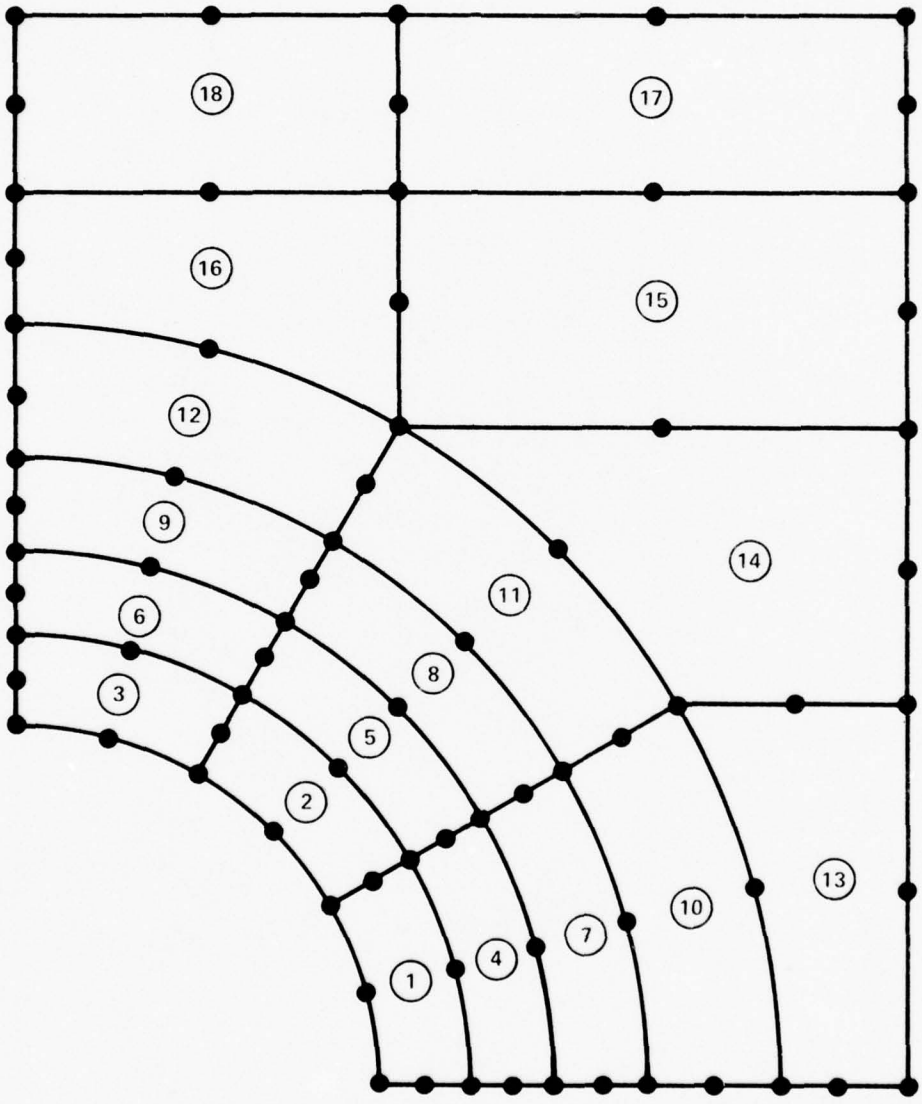

Fig. 4. QUAD-8 Finite Element Model of Unstiffened Center Hole Plate

C.1 Unreinforced hole, stress and minimum limits

The problem was initiated from a uniform design with skin thickness = 0.084 in. A weight of 0.318 lbs. was obtained in 18 iterations. The results given in Table 3 show the large buildup in thickness around the hole.

The design is not fully converged. There are 20 active stress constraints and five active minimum side constraints. The square root of the design factors $\sqrt{I_j}$ are converged to 1.0 $\pm$ 3 percent (with the largest variation in the design variables close to, but not equal to, the minimum area). Therefore, as in the previous examples, continued redesign would not lead to large changes in the design variables or final weight.

C.2 Unreinforced hole, stress, minimum and maximum limits

The large thickness buildup around the unreinforced holes is unrealistic for plate manufacture and may also violate the conditions for plane stress analysis. These difficulties can be minimized by imposing maximum as well as minimum limits on the design variables. The procedure was initiated from a uniform starting design with thickness = 0.084 in. The design problem was modified by imposing a maximum side limit = 0.12 in. on the design variables. A weight of 0.323 lbs. was obtained in 19 iterations with final results as given in Table 4. This weight is as expected greater than the design obtained with no maximum side limits.

The design is fully converged with 21 active stress constraints, one maximum side constraint and six minimum side constraints. The design factors for the elements not constrained by minimum or maximum side limits

TABLE 3

MINIMUM WEIGHT DESIGN OF PLATE WITH UNREINFORCED CENTER HOLE, STRESS AND MINIMUM THICKNESS LIMITS

Variable	Thickness	Variable	Thickness
1	0.1670	16	0.0162
2	0.1064	17	0.0166
3	0.0345	18	0.0230
4	0.0100	19	0.0464
5	0.0100	20	0.0100
6	0.0141	21	0.0141
7	0.0749	22	0.0182
8	0.0729	23	0.0210
9	0.0324	24	0.0235
10	0.0100	25	0.0330
11	0.0107	26	0.0186
12	0.0175	27	0.0251
13	0.0582	28	0.0286
14	0.0459	29	0.0207
15	0.0100	W = 0.3179 lbs.	

TABLE 4

MINIMUM WEIGHT DESIGN OF PLATE WITH UNREINFORCED CENTER HOLE, STRESS, MINIMUM AND MAXIMUM THICKNESS LIMITS

Variable	Thickness	Variable	Thickness
1	0.1200	16	0.0123
2	0.0846	17	0.0143
3	0.0347	18	0.0372
4	0.0100	19	0.0376
5	0.0100	20	0.0100
6	0.0893	21	0.0100
7	0.0762	22	0.0138
8	0.0610	23	0.0196
9	0.0307	24	0.0248
10	0.0100	25	0.0334
11	0.0125	26	0.0186
12	0.0475	27	0.0242
13	0.0534	28	0.0304
14	0.0433	29	0.0213
15	0.0100	W = 0.3229 lbs.	

are identically equal to 1.0, the design factors for the element constrained by the maximum limits is greater than 1.0 and the design factor for the elements constrained by minimum side limits are less than 1.0.

C.3 Reinforced hole, stress and minimum limits

The unrealistic thickness buildup near the hole of the unreinforced plate may also be averted by reinforcing the hole. The reinforcement is modeled by five two-node truss elements. The design process was initiated from a starting design with uniform thickness = 0.804 in. and uniform reinforcement area = 0.36 in^2. A weight of 0.316 lbs. was obtained in 13 iterations; details of this design are given in Table 5. As expected, the presence of the reinforcement causes a reduction in the skin thickness around the hole and the final weight, as compared to the unreinforced case. (However, in all cases, the difference in the design variables and final weights is not large.)

This design is not fully converged. For this problem there are 24 active stress constraints and seven active minimum constraints. The square root of the design factors are converged to 1.0 $\pm$ 2 percent.

TABLE 5

MINIMUM WEIGHT DESIGN OF PLATE WITH REINFORCED CENTER HOLE, STRESS AND MINIMUM THICKNESS LIMITS

Variable	Thickness	Variable	Thickness
1	0.0802	19	0.0387
2	0.1225	20	0.0100
3	0.0418	21	0.0138
4	0.0122	22	0.0178
5	0.0100	23	0.0217
6	0.0244	24	0.0246
7	0.0433	25	0.0262
8	0.0867	26	0.0206
9	0.0356	27	0.0238
10	0.0100	28	0.0262
11	0.0168	29	0.0229
12	0.0232		Area
13	0.0352	30	0.0717
14	0.0618	31	0.0182
15	0.0100	32	0.0100
16	0.0185	33	0.0100
17	0.0195	34	0.0100
18	0.0225	W = 0.3157 lbs.	

IV. OPTIMIZATION INCLUDING FRACTURE CONSTRAINTS

The need to include fracture constraints in structural analysis and design is evidenced by the increasing volume of literature on the subject in a number of structural engineering problems, ranging from nuclear reactor components [12 - 15] to lightweight aircraft components [16 - 20]. However, little work has been done to rationally include fracture constraints in automated structural design. Simultaneous failure concepts were used by Hunt [16] to design stiffened panels. Hunt assumed an optimum minimum weight design would occur when the stress in the frame/crack stopper and the average stress in the skin panel containing the crack simultaneously reached allowable values. Recently, Davis [21] used mathematical programming methods to design an integrally stiffened two-panel box beam with stress, displacement, buckling and fracture constraints, as well as side constraints on the design variables. The design variables were skin thickness and the thickness, depth and spacing of the integral stiffeners. The fracture constraints included limits on developed stress intensity factors under large static loads as well as limits on crack growth during cyclic loads. Analytical results were used for the stress intensity factor under static loads and for the increment in the stress intensity factor under cyclic loads.

The simultaneous failure method of Ref. 16 has limited application since simultaneous failure design may not yield a true optimum design as, for example, when side constraints on the design variables are included. The mathematical programming method of Ref. 21 is capable of converging to true optimum designs, but the method is computationally expensive, even when implemented with analytical results for developed stress intensity

factors. Extension of the method of Ref. 21 to problems requiring numerical calculation of developed stress intensity factors would be computationally prohibitive.

The present optimality criteria method can be used for efficient automated minimum weight design of structural components for which analytic solutions for developed stress intensity factors are not available. The finite element method is used for stress analysis and the strain energy release rate method (the compliance method) is used to calculate developed opening mode stress intensity factors. Only two structural analyses are needed at each design iteration to calculate necessary response gradient information as well as the developed stress intensity factor. The method is applicable to design under large static loads, including fail-safe design of aircraft fuselage panels.

A brief review of the principles of linear elastic fracture mechanics (LEFM) follows, after which is presented the response gradient calculations required to incorporate the fracture mechanics constraints into the design algorithm. Numerical results for a fuselage design problem are used to illustrate the importance of fracture mechanics constraints.

A. Irwin Theory of Linear Elastic Fracture Mechanics

Irwin [22] has shown that a general linear elastic stress state asymptotically close to a crack tip is a linear combination of three distinct stress states, each stress state associated with a particular mode of crack tip deformation. The three deformation modes are Mode I, the opening mode in which the crack surfaces separate in a direction normal to the crack surface; Mode II, the sliding mode in which the crack surfaces

slide along a direction perpendicular to the crack front; and, Mode II, the tearing mode in which the crack surfaces slide in a direction parallel to the crack front.

The near crack tip stresses and displacements in each mode have been obtained using complex variable techniques [23] and eigenfunction expansions [24]. The near crack tip results are the product of an intensity factor and functions of the position coordinates. The results for Mode I deformation of an infinitely sharp crack are

$$\begin{Bmatrix} \sigma_{xx} \\ \sigma_{yy} \\ \tau_{xy} \end{Bmatrix} = \frac{K_I}{\sqrt{2\pi r}} \cos\left(\frac{\theta}{2}\right) \begin{Bmatrix} 1 - \sin\left(\frac{\theta}{2}\right)\sin\left(\frac{3\theta}{2}\right) \\ 1 + \sin\left(\frac{\theta}{2}\right)\sin\left(\frac{3\theta}{2}\right) \\ \sin\left(\frac{\theta}{2}\right)\cos\left(\frac{3\theta}{2}\right) \end{Bmatrix} \tag{23}$$

$$\begin{Bmatrix} u \\ v \end{Bmatrix} = \frac{K_I}{2\mu}\sqrt{\frac{r}{2\pi}} \begin{Bmatrix} \cos\left(\frac{\theta}{2}\right)\left[\kappa - 1 + 2\sin^2\left(\frac{\theta}{2}\right)\right] \\ \sin\left(\frac{\theta}{2}\right)\left[\kappa + 1 - 2\cos^2\left(\frac{\theta}{2}\right)\right] \end{Bmatrix} \tag{24}$$

where K_I is the opening mode stress intensity factor and x and y are cartesian coordinates and r and θ are polar coordinates with origin at the crack tip (Fig. 5). In Eq. (24), u and v are the displacements along x and y, respectively, μ is the elastic shear modulus and

$$\kappa = \begin{cases} (3 - 4\nu), & \text{plane strain} \\ (3 - \nu)/(1 + \nu), & \text{generalized plane stress} \end{cases} \tag{25}$$

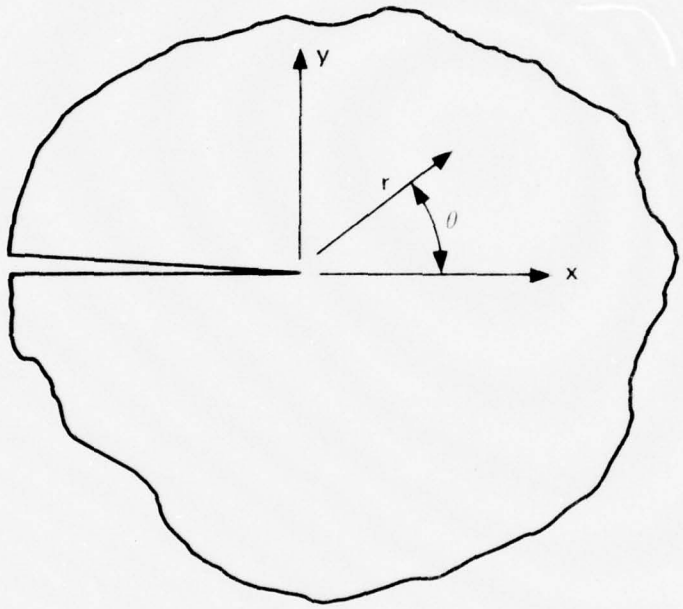

Fig. 5. Geometry of Region Near Crack Tip

These results are valid only for $r \ll c$ where c is the crack half-length.

The stress intensity factor K_I controls the intensity of the elastic stresses near the crack tip. For a small extent of yielding at the crack tip, the elastic stresses outside the plastic zone are not greatly disturbed and are completely described by the stress intensity factor. Therefore, the stress intensity factor is the relevant fracture parameter for elastic and limited yielding fracture.

The value of the stress intensity factor is dependent on the loading and specimen geometry and is obtained by an analytical or numerical solution of the boundary value problem. Thus, the near crack tip stresses are the same for different boundary conditions if the stress intensity factors are the same.

The criterion for the onset of fracture is that the state of stress at the crack tip reaches a critical state, or equivalently, that the stress intensity factor reaches a critical value. Therefore, for the opening mode, fast fracture first occurs when

$$K_I = K_C \tag{26}$$

where K_C is the critical opening mode stress intensity factor.

Experimental results show the critical opening mode stress intensity factor to be primarily dependent on specimen thickness and the state of stress at the crack tip. For thick test specimens, predominantly in a state of plane strain, the critical opening mode stress intensity factor is a material constant and is denoted K_{IC}. The critical plane strain

stress intensity factor can be measured for one carefully controlled loading and geometry. The corresponding critical state of near-crack-tip stresses is the same for all other cases of loading and geometry.

For test specimens not predominantly in a state of plane strain the critical opening mode stress intensity factor is not constant, but increases with decreasing thickness. The critical state of stress is not independent of the boundary conditions. Therefore, the test specimen and the service specimen must be of similar geometry and size.

B. Solution for Developed Stress Intensity Factors

A number of methods can be used to solve for developed stress intensity factors (given the finite element solution of the boundary value problem. These methods include:

(1) stress matching;

(2) displacement matching;

(3) energy release; and

(4) embedded singularity.

These methods are briefly reviewed with an emphasis on the calculation of the developed opening mode stress intensity factor K_I.

B.1 Stress matching

In this method, corresponding values of the stresses and position coordinates are substituted into the singular solution, Eq. (23), to solve for the stress intensity factor K_I. It has been found most accurate to use the tensile component of stress σ_{xx} with $\theta = 0$ (then $r = x$, the

distance along the x-axis). Apparent stress intensity factors K_I^* are calculated from Eq. (23a) with $\theta = 0$,

$$K_I^* = \sigma_{xx} \sqrt{2\pi r} \quad . \tag{27}$$

If the stresses from the finite element analysis were exact, then a unique value of K_I^* would result. However, extrapolation is necessary since non-singular finite element analysis is not exact near the crack tip. Plotting K_I^* as a function of r and extrapolating the linear portion of the relationship to $r = 0$ gives an estimate of the stress intensity factor at the crack tip.

The extrapolation can be used only if there is an overlapping range of validity of the singular solution, Eq. (23a), and of the finite element solution. An overlapping range of validity is obtained only by extending the range of the numerical solution near the crack tip by using a fine and computationally costly finite element grid.

B.2 Displacement matching

The displacement matching method is similar to the stress matching method. Corresponding values of displacements and position coordinates are substituted into Eq. (24) to solve for K_I. It has been found most accurate to use the vertical component of the displacement v with $\theta = \pi$ so that

$$K_I^* = \frac{2\mu v}{(\kappa + 1)} \sqrt{\frac{2\pi}{r}} \quad . \tag{28}$$

Extrapolation to $r = 0$ gives an estimate of the stress intensity factor at the crack tip.

B.3 Energy release

The relation between linear elastic strain energy release rate G and the Mode I stress intensity factor K_I is

$$G = \left| \pm \frac{\partial U}{\partial A} \right| = \frac{\alpha K_I^2}{E} \tag{29}$$

where $U = \frac{1}{2} \{F\}^T \{u\}$ is the strain energy, A is the projected crack area and

$$\alpha = \begin{cases} 1.0 \ , & \text{generalized plane stress} \ , \\ 1.0 - \nu, & \text{plane strain} \ . \end{cases} \tag{30}$$

For "fixed grips," $G = -\partial U/\partial A$, with $\partial U/\partial A < 0$ and the energy for the formation of new crack surfaces is provided by the decrease in the strain energy of the body as a result of crack propagation. For fixed boundary forces, $G = \partial U/\partial A$, with $\partial U/\partial A > 0$ and the energy for the formation of new crack surfaces is provided by the decrease in potential energy of the external loads due to crack propagation.

The energy release rate can be evaluated in two ways: (1) the compliance difference [25]; and (2) the Rice J-integral [26]. In the compliance difference method, the release rate G is calculated by replacing the partial differential operator, $\partial/\partial A$ in Eq. (29), by the finite difference operator $\Delta/\Delta A$ and measuring the strain energy of the body with two different crack areas. In the Rice J-integral method, the release rate is related to the path independent J-integral

$$J = \int_{\Gamma} \left(u\, dy - \bar{T} \cdot \frac{\partial \bar{u}}{\partial x}\, ds \right) \equiv G \qquad (31)$$

where u is the strain energy density, $\bar{T}$ is the traction vector, $\bar{u}$ is the displacement vector, x and y are the cartesian coordinates with origin at the crack tip, Γ is the integral path surrounding the crack tip and ds is an element of the arc along Γ.

The advantage of the energy release rate method is that fine finite element grids are not required at the crack tip. The Rice J-integral method requires only one structural analysis to calculate G, while the compliance method requires two analyses.

B.4 Embedded singularity

In this method singular near crack tip elements are used with non-singular elements to model the stress singularity at the crack tip. Two types of singular elements are used, cracked elements and collapsed elements. With cracked elements the stress intensity factor is a degree of freedom of the system and is obtained directly by solving the equilibrium equations. With collapsed elements the stress intensity factor is obtained indirectly by displacement matching.

For numerical calculations of developed stress intensity factors in single mode problems, the energy release rate methods are best. Stress and displacement matching require fine finite element grids near the crack tip, while the embedded singularity methods require special singular elements at the crack tip. For analysis, the release rate calculation by the Rice J-integral is best since only one structural analysis is required.

However, for design, the compliance method is best since a minimum of two analyses are already required for gradient calculations, and integration along a path around the crack tip is not required as with the J-integral.

C. Fracture Constraint Gradient Calculations

Developed opening mode stress intensity factors at the crack tip are calculated using the linear eleastic strain energy release rate method (the compliance method). As was already mentioned, for numerical calculations the partial derivative operator $\partial/\partial A$ in Eq. (29) is replaced by the finite difference operator $\Delta/\Delta A$ and G is obtained by taking the difference in strain energy of the body with two different crack lengths, A_1 and $A_2 = A_1 + \Delta A$ (the derivative applies to a mean crack length $A = (A_1 + A_2)/2$). Therefore, two complete structural analyses are needed. These two analyses also provide all required constraint gradient information.

Differentiating Eq. (29) with respect to the design variables gives

$$\frac{\partial G}{\partial D_j} = \frac{2\alpha K_I}{E} \frac{\partial K_I}{\partial D_j} \quad , \tag{32}$$

from which

$$\frac{\partial K_I}{\partial D_j} = \frac{E}{2\alpha K_I} \frac{\partial G}{\partial D_j} \quad . \tag{33}$$

For the case of fixed forces,

$$\frac{\partial G}{\partial D_j} = \frac{1}{2} \{F\}^T \frac{\partial}{\partial D_j} \left(\frac{\partial \{u\}}{\partial A} \right) + \frac{1}{2} \frac{\partial \{F\}^T}{\partial D_j} \frac{\partial \{u\}}{\partial A}$$

$$= \frac{1}{2} \{F\}^T \frac{\partial}{\partial A} \left(\frac{\partial \{u\}}{\partial D_j} \right) \quad . \tag{34}$$

Substituting Eq. (34) into Eq. (33) gives

$$\frac{\partial K_I}{\partial D_j} = \frac{E}{4\alpha K_I} \{F\}^T \frac{\partial}{\partial A}\left(\frac{\partial \{u\}}{\partial D_j}\right)$$

$$\cong \frac{E}{4\alpha K_I} \{F\}^T \frac{\Delta}{\Delta A}\left(\frac{\partial \{u\}}{\partial D_j}\right) . \qquad (35)$$

At the beginning of each redesign iteration the displacements, displacement gradients and strain energy are calculated with crack area $A = A_2$. The developed opening mode stress intensity factor is obtained by closing the crack so that $A = A_1 = A_2 - \Delta A$, calculating the displacements and strain energy and completing the calculation of Eq. (29). (The crack front is closed by suppressing one or more nodes along the crack line; the stiffness matrix and stiffness gradients at $A = A_1$ are obtained by imposing the boundary conditions corresponding to the closed nodes on the stiffness matrix and stiffness gradients at $A = A_2$.) If the fracture constraint is active, then the displacement gradients at $A = A_1$ are obtained and the fracture constraint gradient calculation of Eq. (35) is completed. Gradients of active displacement and stress constraints are obtained only at $A = A_1$.

D. Numerical Results

As a typical example, the design of a center cracked stiffened aircraft fuselage panel is considered. The crack is assumed to lie between two frame members in a symmetric manner so that only a quarter of the panel need be considered (Fig. 6). A uniform tensile stress, approximately equal to the hoop stress of a pressurized DC-10 fuselage panel [17, 18, 19] is applied.

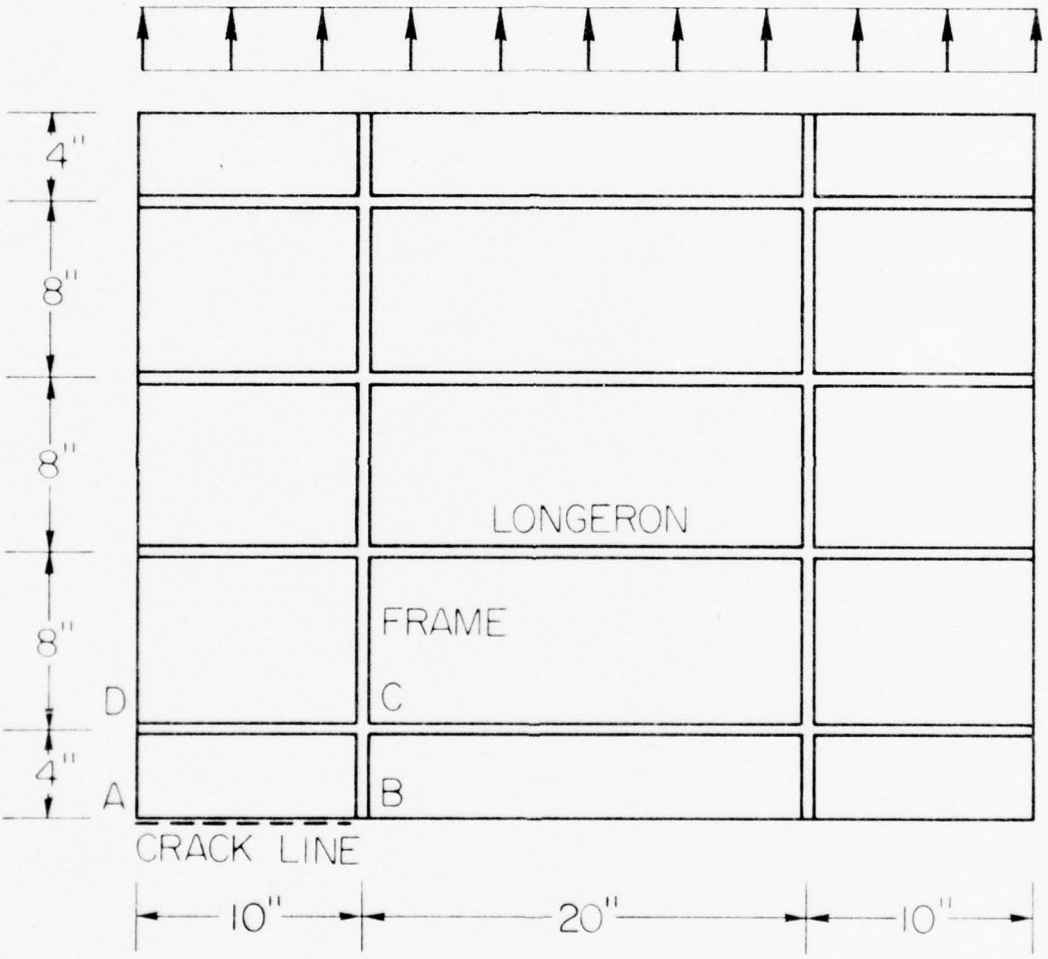

Fig. 6. Quarter Section of Center Cracked Panel

The finite element grid for the skin panel containing the crack is shown in Fig. 7 (region ABCD as shown in Fig. 6). A total of 152 finite elements is used to model the stiffened panel; 14 two-node truss elements to model the frame, 33 truss elements to model the longerons and 50 planar three-node triangles and 55 planar isoparametric quadrilaterals to model the skin panels. The 152 finite elements are linked to three independent design variables. The 14 truss elements are linked to D_1 (the frame area), the remaining 33 truss elements are linked to D_2 (the longeron area) and the 105 planar elements are linked to D_3 (the skin thickness).

The frame and longeron material is Aluminum 2024-T3 with elastic modulus $E = 10 \times 10^6$ psi., Poisson ratio $\nu = 0.3$, specific weight $\rho = 0.1$ pci., and yield stress $\sigma_y = \pm 57.0 \times 10^3$ psi. The skin material is Aluminum 7075-T6 with $\sigma_y = \pm 80.0 \times 10^3$ psi. The variation of the critical opening mode stress intensity factor K_C with thickness for Aluminum 7075-T6 is shown in Fig. 8 [27]. (Secondary effects such as specimen width, stiffener spacing, etc., are neglected.) For thicknesses less than approximately 0.45 in. K_C is constant and approximately equal to 57.0×10^3 psi.$\sqrt{\text{in.}}$ The plane strain critical opening mode stress intensity factor is taken to be 27.0×10^3 psi.$\sqrt{\text{in.}}$ for thicknesses greater than approximately 1.0 in.

The fail-safe structural integrity requirement specifies the residual strength of the cracked panel to be sufficient to arrest the crack and permit damage detection in a "walk around" inspection [20]. The residual strength or residual stress is the applied stress required to cause fast fracture of an existing crack of a given length. The residual stress σ_r

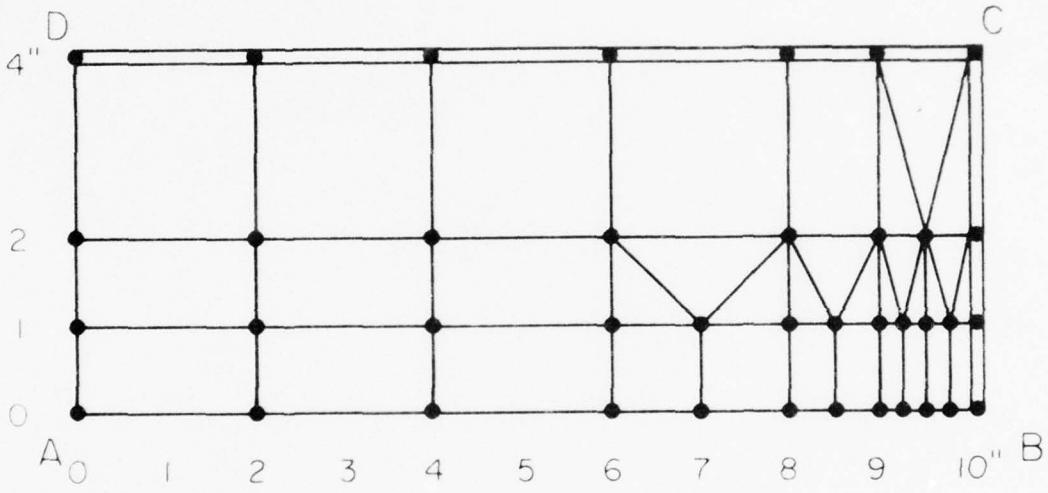

Fig. 7. Finite Element Idealization of Skin Panel Containing Crack Shown in Fig. 1

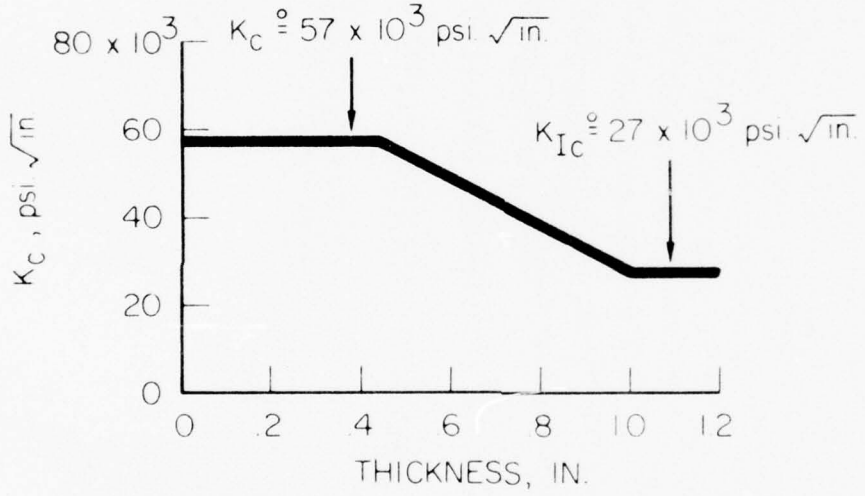

Fig. 8. Variation of Critical Stress Intensity Factor with Thickness

of an unstiffened panel decreases with increasing crack length; therefore, any crack which propagates rapidly will not be arrested and will continue to propagate. The residual stress of a stiffened panel initially decreases with increasing crack length but then increases as the crack approaches the frame member since the frame member relieves the stress at the crack tip. Thus, a fast propagating crack in a stiffened panel may be arrested if the frame members are sufficiently stiff.

The increase in the stress in the frame member as the crack approaches the frame may cause failure by yielding of the frame material. Thus, two distinct failure mechanisms are operative, fast fracture of the skin (the skin criterion) and yielding of the frame (the frame criterion). Both failure mechanisms must be prevented in a fail-safe design.

The residual stress for the center cracked panel with initial design $D_1 = 0.5$ in.^{2}, $D_2 = 0.3$ in.^{2} and $D_3 = 0.07$ in. is shown in Fig. 9. (The initial design approximates test panels of Refs. 17, 18 and 19.) The residual stresses for both the skin and the frame are shown. (For comparison purposes, the residual stress for the skin of an unstiffened panel with skin thickness = 0.07 in. is also shown.) Clearly, the frame failure mechanism will not be active in this initial design.

(The residual stress curves were obtained by closing the crack face, successively suppressing one node at a time along the crack line, and calculating the strain energy for each crack length. Developed stress intensity factors were compared to the critical stress intensity factor and the applied stress scaled to cause fast fracture of the crack. The finite element grid is finer near the frame than near the center line of the panel because of the increasing influence of the frame on the approaching crack.

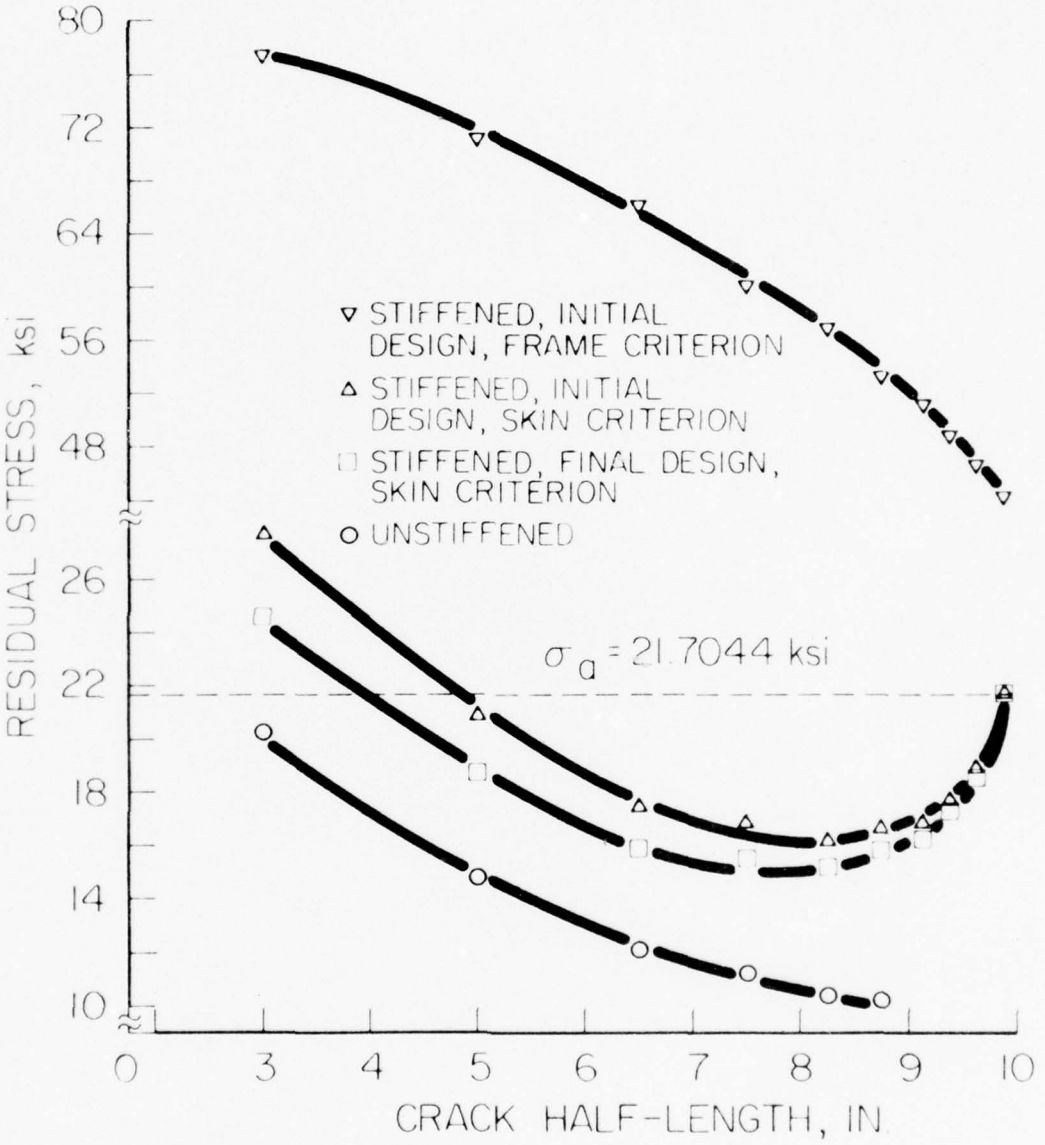

Fig. 9. Residual Stress of Center Cracked Panel

Thus, the residual stress calculations are more accurate near the frame because of the smaller crack length increments used to determine the gradients.)

The residual stress usually attains a maximum value when the crack just propagates past the frame centerline with the (fastened) frame remaining intact. This situation cannot easily be simulated in the present study because truss elements are used to model the frame members. Therefore, the maximum residual stress is assumed to occur with crack half-length $a = (10.0 + 9.75)/2.0 = 9.875$ in., the maximum crack length that can be considered. The uniformly applied tensile stress is scaled so that the developed stress intensity factor with $a = 9.875$ in. was equal to the critical value $K_C = 57.0 \times 10^3$ psi.$\sqrt{\text{in.}}$ This scaling gives an applied stress $\sigma_a = 21{,}704.4$ psi.

A line of constant stress equal to the applied stress intercepts the residual stress curve (Fig. 9) at $a = 9.875$ in. and $a \cong 5.0$ in. Thus, $a = 5.0$ in. is the length of the longest crack which will be arrested at the applied stress, and is denoted a_t, the threshold crack length [28]. Longer cracks with $a > a_t$ will be arrested if the applied stress is less than $\sigma_a = 21{,}704.4$ psi.

The optimum design problem is stated as follows: minimize the weight of the stiffened panel while maintaining for crack length $a = 9.875$ in. the residual stress greater than or equal to the applied stress $\sigma_a = 21{,}704.4$ psi., or equivalently, maintain with $a = 9.875$ in., $K_I \geq K_C$. Stress constraints on longeron and skin yielding were included as well as the stress constraints on frame yielding. The initial design with $D_1 = 0.5$ in.^{2}, $D_2 = 0.3$ in.^{2}, and $D_3 = 0.07$ in. weighed 16.96 lbs.

Minimum limits on the design variables were arbitrarily chosen (72 percent of the initial values); maximum limits were not imposed.

The final design with $D_1 = 0.688$ in.^{2}, $D_2 = D_{2_{min}} = 0.216$ in.^{2} and $D_3 = D_{3_{min}} = 0.0504$ in. weighed 14.33 lbs. This final design is fully converged with the design factors (Eq. 9) $I_1 \equiv 1.0$, $I_2 < 1.0$ and $I_3 < 1.0$ and was obtained in seven iterations (requiring approximately 16 CPU seconds for execution on the UCLA Campus Computing Network IBM 360/91 computing system with single precision arithmetic and the FORTRAN G compiler). Only the fracture constraint was active during the design process.

The frame relieves the stress at the crack tip and reduces the developed opening mode stress intensity factor at the crack tip. For the initial design, $\partial g_1/\partial D_1 = -0.891$ where $g_1 = K_I/K_C - 1.0$ is the constraint on the developed stress intensity factor. Increasing the skin thickness is nearly as effective in decreasing the developed stress intensity factor at the crack tip as increasing the frame area; for the initial design $\partial g_1/\partial D_3 = -0.779$. However, increasing the skin thickness has a greater effect on weight than increasing the frame area since $W = \rho \sum_{j=1}^{3} (\partial W/\partial D_j) D_j$ where $\partial W/\partial D_1 = 6.40$ and $\partial W/\partial D_3 = 128.0$ (the weight gradients are constant). For a given value of the Lagrange multiplier λ associated with the fracture constraint, the design factor $I_1 \cong 23\, I_2$ and $\sqrt{I_1} \cong 4.8 \sqrt{I_2}$ or $\sqrt{I_2} \cong .208 \sqrt{I_1}$. Thus, by Eqs. 10 and 11, the skin and the longerons, which have little effect on the developed stress intensity factor, are quickly reduced to minimum value. The minimum value chosen for the skin will have a large effect on final weight.

The residual stress curve for the final design is shown in Fig. 9. Only the skin criterion is active. The threshold crack length for the final design with σ_a = 21,704.4 psi is $a_t \cong 4.0$ in. Thus, the optimization decreases the panel weight (approximately 15.5 percent) but also decreases the threshold crack length, the length of crack which will just be arrested at the applied load. Durability requirements of the type proposed in Ref. 20 can also be included in the present optimization algorithm. For details see Appendix D.

E. Discussion

The results for the center cracked stiffened panel show that significant weight decreases are possible while maintaining the structural integrity of the panel. Similar results were obtained for a center hole cracked stiffened panel (modeled by deleting the longeron four inches above the crack line of the center crack model and inserting an eight inch diameter hole). Again, the weight decrease is obtained at the cost of an increased sensitivity to initial crack sizes (i.e., a decrease in threshold crack lengths).

The criteria for fracture resistant aircraft structures proposed in Ref. 20 includes a durability requirement as well as a structural integrity requirement. The structural integrity requirement ensures that cracks will not grow to critical size during the life span of the structure. For example, the durability requirement proposed in Ref. 20 for fail-safe design states that an initial crack of half length a = 0.125 in. not grow to critical size in two life spans of the aircraft. The growth rate is calculated ignoring structural design details. This requirement ensures against expensive repair of a panel failure during the life span of the

the aircraft. Durability requirement constraints can be included in the present method at some additional computational cost.

The results of the present study were obtained by modeling the frame and longerons only by truss members. More accurate results could be obtained by a more detailed modeling of the frame and longerons and their connections to the sheet. Improved modeling would permit study of crack stoppers and frame members of different materials and allow consideration of secondary effects such as stringer eccentricity, rivet spacing, etc. [1, 28]. This more detailed (and more costly) modeling would allow consideration of more practical cases where cracks span two skin panels, since cracks usually do not start at the middle of a panel but, rather, start at stiffener attachments and run into one or both adjacent skin panels.

The present results were obtained with the total number of finite elements linked to three independent design variables. Improved results may be expected if a less severe linking were imposed and a larger number of design variables were considered, especially near probable crack locations.

The designs obtained by the present method are based on the existence of a crack at a specified location and with a specified geometry and assumed opening mode tip deformation. Several cracks at different locations should be postulated for a more realistic application of this method. A finite element analysis for each crack could be implemented and included in the present design algorithm. Thus, the method can be applied to a wide range of design problems requiring the inclusion of fracture

constraints.

Finally, it should be noted that for this problem the fracture mechanics constraint was the dominant design consideration, i.e., stress and displacement constraints were not active. For other applications it is clear that stress, displacement and side constraints may become active, but clearly, design for fracture prevention is a very important effect and must be incorporated in automated structural design.

V. CLOSURE

The primary research objective in the study of optimality criteria approach to automated structural design has been to develop an efficient design algorithm capable of treating large structural systems with several hundred or more design variables. In addition, the algorithm has been developed with a capability for dealing with minimum weight design problems involving stress, displacement, side constraints on other design variables and constraints against fracture.

As described in this Interim Report these objectives have been attained. The present algorithm is capable of determining very efficient designs of a wide range of aerospace structures, subjected to multiple static load systems and constrained against several forms of inadmissable behavior. The algorithm has been tested with several well known difficult elastic-truss design problems and has also been exercised on design problems involving built up assemblages of two-dimensional stiffened panel structures.

The present algorithm has been shown to produce near optimum designs with a significantly smaller computer effort than the best available mathematical programming techniques. Although the present algorithm does require more computational effort than other heuristic "optimality" criteria methods (since the algorithm is based on the true mathematical optimality criteria, the Kuhn-Tucker test), the designs produced by the algorithm are at a local optimum point. This capability has been shown [1] to produce designs which are superior to designs developed using the heuristic optimality criteria methods.

Perhaps the most important aspect of the research reported herein is the development of an automated structural design capability for treating constraints against fast fracture due to propagation of existing structural cracks. As indicated by the results in Section IV, the inclusion of fracture mechanics constraints can have a dominant effect on optimum structural design since the structures designed with this constraint included were not constrained by the more conventional maximum and/or minimum limits on allowable displacements and stresses. Based on these results, it is recommended that research continue in the area of automated design of aircraft structures for fracture resistance and safe-life requirements.

REFERENCES

[1] Dobbs, M.W., and R.B. Nelson, "Application of Optimality Criteria to Automated Structural Design," AIAA Journal, Vol. 14, No. 10, October 1976.

[2] Venkayya, V.B., Khot, N.S., and V. S. Reddy, "Optimization of Structures Based on the Study of Energy Distribution," AFFDL-TR-68-150, Air Force Flight Dynamics Laboratory, March 1969.

[3] Kiusalaas, J., "Minimum Weight Design of Structures Via Optimality Criteria," NASA TN D-7115, 1972.

[4] Berke, L., and N.S. Khot, "Use of Optimality Criteria Methods for Large Scale Systems," AGARD Lecture Series, No. 70 on Structural Optimization, AGARD-LS-70, 1974.

[5] Berke, L., and V.B. Venkayya, "Review of Optimality Criteria Approaches to Structural Optimization," ASME Structural Optimization Symposium, AMD Vol. 7, 1974.

[6] Wilde, D.J., and C.S. Beightler, Foundations of Optimization, Prentice Hall, Englewood Cliffs, N.J., 1967.

[7] Dobbs, M.W., and R. B. Nelson, "Application of Optimality Criteria to Stress Limited Structural Design," AFOSR-TR-75-1431, 1975.

[8] Rizzi, P., "The Optimization of Structures with Complex Constraints Via a General Optimality Criteria Method," Ph.D. Dissertation, Stanford University, Stanford, California, 1976.

[9] Terai, K., "Application of Optimality Criteria in Structural Synthesis," UCLA-ENG-7446, School of Engineering and Applied Science, University of California, Los Angeles, California, 1974.

[10] Schmit, L.A., and H. Miura, "Approximation Concepts for Efficient Structural Synthesis," NASA CR-2552, 1975.

[11] Pope, G.G., "Optimum Design of Stressed Skin Structures," AIAA Journal, Vol. 11, No. 11, September 1973.

[12] Kiss, E., Heald, J.D., and D.A. Hale, "Fatigue Crack Growth in Prototype Piping and Components," Symposium on the Technology of Pressure Retaining Steel Components, Vail, Colorado, 1970.

[13] Rowe, G.H., "Matrix Displacement Methods in Fracture Mechanics Analysis of Reactor Vessels," First International Conference on Structural Mechanics in Reactor Technology, Berlin, 1971.

[14] Bergan, P.G., and B. Aamodt, "Finite Element Analysis of Crack Propagation in Three Dimensional Solids Under Cyclic Loading," Second International Conference on Structural Mechanics in Reactor Technology, Berlin, 1973.

[15] Bartholome, G., Miksch, M., Neubrech, G., and G. Vasoukis, "Fracture and Safety Analysis of Nuclear Pressure Vessels," Engineering Fracture Mechanics, Vol. 4, 1973.

[16] Hunt, R.T., "Crack Propagation and Residual Static Strength of Stiffened and Unstiffened Sheet," Current Aeronautical Fatigue Problems, ed., Schijve, J., Heath-Smith, J.R., and E.R. Welbourne, Pergamon Press, 1965.

[17] Swift, T., and D.Y. Wang, "Damage Tolerant Design-Analysis Methods and Test Verification of Fuselage Structure," Proceedings of the Air Force Conference on Fatigue and Fracture of Aircraft Structures and Materials, AFFDL-TR-70-144, 1970.

[18] Swift, T., "Development of the Fail-Safe Design Features of the DC-10," Damage Tolerance in Aircraft Structures, ASTM STP486, 1971.

[19] Swift, T., "The Application of Fracture Mechanics in the Development of the DC-10 Fuselage," Fracture Mechanics of Aircraft Structures, ed., Liebowitz, H., AGARD-AG-176, 1974.

[20] Ekvall, J.C., Brussat, T.R., Liu, A.F., and M. Creager, "Engineering Criteria and Analysis Methodology for the Appraisal of Potential Fracture Resistant Primary Aircraft Structure," AFFDL-TR-72-80, 1972.

[21] Davis, C.S., "Inclusion of Crack Growth and Fracture Constraints in Automated Design," Doctoral Dissertation, School of Engineering and Applied Science, University of California, Los Angeles, California, 1976.

[22] Irwin, G.R., "Fracture Mechanics," Structural Mechanics, eds., Goodier, J.N., and N.J. Hoff, Pergamon Press, 1960.

[23] Westergaard, H.M., "Bearing Pressures and Cracks," Journal of Applied Mechanics, Vol. 61, 1939.

[24] Williams, M.L., "Stress Distribution at the Base of a Stationary Crack," Journal of Applied Mechanics, Vol 24, 1957.

[25] Watwood, V.B., "The Finite Element Method for Prediction of Crack Behavior," Nuclear Engineering and Design, Vol. 11, 1969.

[26] Rice, J.R., "A Path Independent Integral and the Approximate Analysis of Strain Concentration by Notches and Cracks," Journal of Applied Mechanics, Vol. 35, 1965.

[27] Allen, F.C., "Effect of Thickness on the Fracture Toughness of 7074 Aluminum in the T6 and T73 Conditions," Damage Tolerance in Aircraft Structures, ASTM STP486, 1971.

[28] Vlieger, H., "The Residual Strength Characteristics of Stiffened Panels Containing Fatigue Cracks," Engineering Fracture Mechanics, Vol. 5, 1973.

[29] Zienkiewicz, O.C., The Finite Element Method in Engineering Science, McGraw-Hill, London, 1971.

[30] Paris, P.C., and F. Erdogan, "A Critical Analysis of Crack Propagation Laws," J. Bas. Engr., Trans. ASME, Series D, Vol. 85, 1963.

APPENDIX A

PROGRAM DOCUMENTATION

A computer program for efficient minimum weight design of large scale structural systems is described in this section. The program utilizes finite elements for stress analysis and the Kuhn-Tucker necessary conditions for design.

Five types of finite elements are applied to the stress analysis. These are:

(1) the three-dimensional, two-node truss element (TRUSS2);

(2) the three-dimensional, three-node subparametric truss element (TRUSS3);

(3) the planar isotropic three-node constant strain triangle (CST);

(4) the planar isotropic four-node isoparametric quadrilateral (QUAD4); and

(5) the planar isotropic eight-node isoparametric quadrilateral (QUAD8).

Details for the stiffness matrix calculations are given in Appendix C.

Four types of behavioral constraints are included in the present version of the design program. These are:

(1) limits on the tensile and compressive stresses in the truss elements and limits on the von Mises equivalent stresses in the planar elements;

(2) limits on nodal displacements;

(3) limits on relative nodal displacements; and

(4) limits on developed opening mode stress intensity factors.

In addition, minimum and maximum side limits on the design variables are included.

The program has 91 subroutines including the main subroutine. All routines are written in FORTRAN IV. Only internal storage is used. All arrays are included in a single blank common; the length of each array is dynamically allocated in terms of the pertinent input parameters. In addition, there are 22 labeled common blocks. All real variables and constants are declared as single precision numbers.

Program Structure

The structure of the program is illustrated in Fig. A1. Subroutine MAIN is listed in Fig. A2. Overall control of the analysis and design is accomplished in MAIN. All control transfers are returned to MAIN.

The four major functions of the program are: (1) data input; (2) analysis; (3) constraint evaluation; and (4) redesign. The first major function, data input, is accomplished in the steering subroutine DATAIN. Besides data input, DATAIN accomplishes the dynamic allocation of all arrays and the calculation of the stiffness gradients (and storage in compacted form).

The second major function is a finite element stress analysis, including, when specified, the calculation of developed opening mode stress intensity factors by the compliance method. The system stiffness matrix is synthesized in STIFF, the system displacements calculated in GLDISP and the member stresses calculated in STRESS. If fracture constraints are active (IACTIV(4)=1) then two analyses are required, one analysis with crack area A_2 and the other analysis with crack area $A_1 = A_2 - \Delta A$.

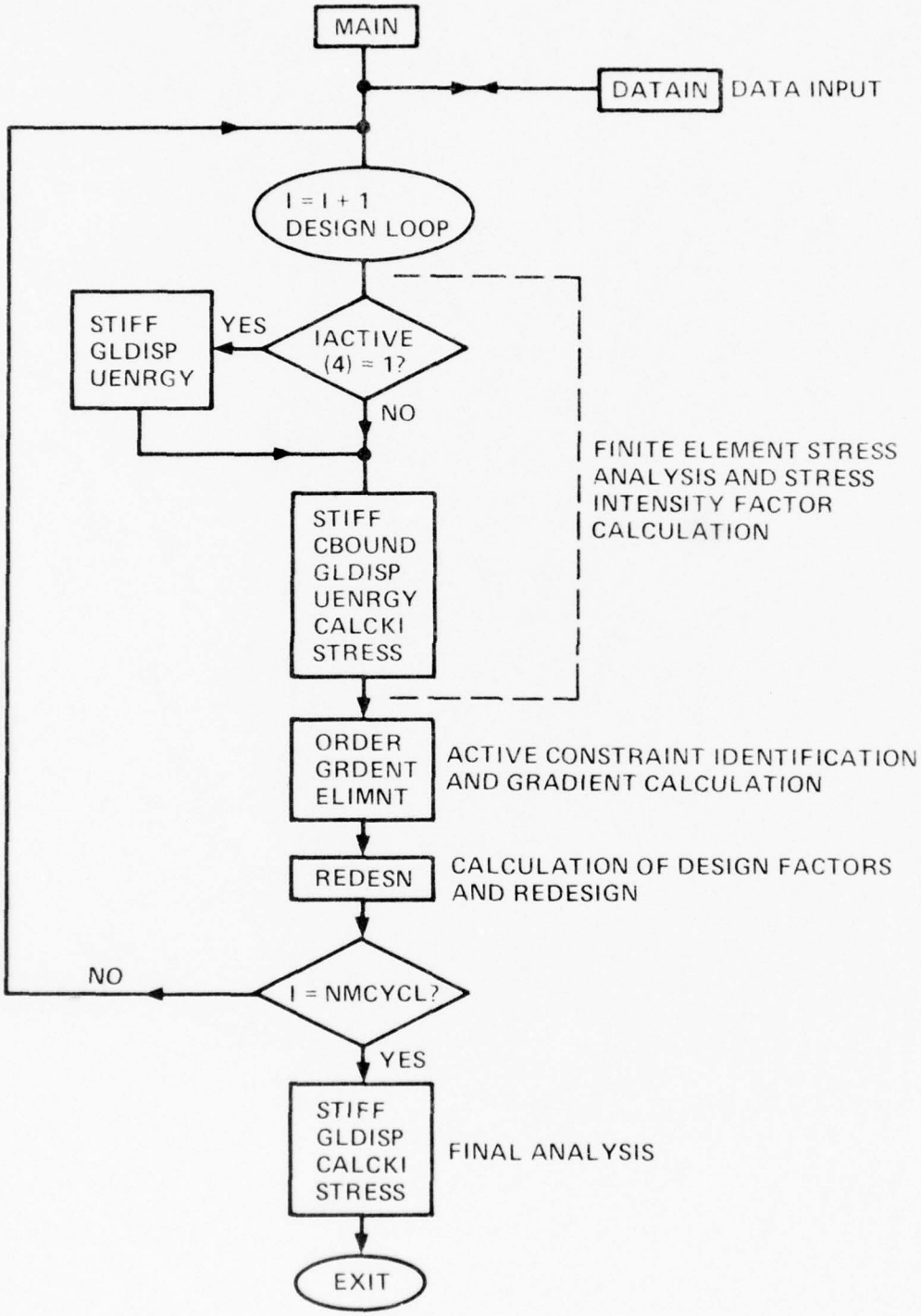

Fig. A1. Program Structure

```
C
C
C     ITERATIVE DESIGN OF STIFFENED PLATES
C     (REFERENCE FOR STATIC STRESS ANALYSIS -- SAP2 BY E.L. WILSON)
C
C
C     IF IACTIV(4)=1, FRACTURE MECHANIC CONSTRAINTS CALCULATED:
C          1.  STRESS INTENSITY FACTOR BY STRAIN ENERGY RELEASE RATE;
C          2.  OPENING MODE DEFORMATION ONLY; AND,
C          3.  TRACTION FREE CRACK SURFACES.
C
C
0001        COMMON              A(35000)
0002        COMMON /CONST /     N1          ,N2         ,N3         ,
           *                    N4          ,N5         ,N6         ,
           *                    N7          ,N8         ,N9         ,
           *                    N10         ,N11        ,N12        ,
           *                    N13         ,N14        ,N15        ,
           *                    N16         ,N17        ,N18        ,
           *                    N19         ,N20        ,N21        ,
           *                    N22         ,N23        ,N24        ,
           *                    N25         ,N26        ,N27        ,
           *                    N28         ,N29        ,N30        ,
           *                    N31         ,N32        ,N33        ,
           *                    N34         ,N35        ,N36        ,
           *                    N37         ,N38        ,N39        ,
           *                    N40         ,N41        ,N42        ,
           *                    N43         ,N44        ,N45        ,
           *                    N46         ,N47        ,N48        ,
           *                    N49         ,M23        ,L23        ,
           *                    K23         ,J23        ,M41        ,
           *                    L41         ,K41        ,J41
0003        COMMON /MINPUT/     NMNODS      ,NMELTP     ,NMELMT     ,
           *                    NMDESV      ,NMLDCN
0004        COMMON /MSIZE /     NEQLA       ,NBAND      ,MAX        ,
           *                    MIN
0005        COMMON /ALLCTE/     NLOAL       ,NLINK      ,NSTRS      ,
           *                    NDISP       ,NCONS      ,NACTS      ,
           *                    NSTIF       ,NRELA      ,NQ
0006        COMMON /SHUTCN/     KSTOP       ,KLAST
0007        COMMON /CHECK /     NZERO       ,NONE       ,NTWO       ,
           *                    ZERO        ,ONE        ,TWO
0008        COMMON /ACHECK/     NTHREE      ,NFIVE      ,NTEN
0009        COMMON /PRINTS/     IPAREA      ,IPDISP     ,IPSTRS     ,
           *                    IPCONS      ,IPGRAD     ,LPAREA     ,
           *                    LPDISP      ,LPSTRS     ,LPCONS
0010        COMMON /ACTIVE/     IACTIV(4)   ,NELOPT
0011        COMMON /CRACK /     CRITKI      ,CRACKA     ,CRACKE     ,
           *                    SYMMET      ,ALPHA      ,NCRACK     ,
           *                    NCGEN       ,NINTH      ,NUP
0012        NZERO           =   0
0013        NONE            =   1
0014        NTWO            =   2
0015        NTHREE          =   3
```

Fig.A2 Main Subroutine (1of3)

```
FORTRAN IV G LEVEL  21                    MAIN                    DATE = 77047          13/32/38                    PAGE

0016                NEIVE          =        5
0017                NTEN           =        10
0018                ZERO           =        0.0
0019                ONE            =        1.0
0020                TWO            =        2.0
0021              5 CONTINUE
0022                CALL DATAIN (NMCYCL)
0023                IF (KSTOP .EQ.NONE  ) GO TO 10
0024                PRINT 2002
0025                DO 15 I=1,NMCYCL
0026                PRINT 2000, I
0027                CALL PRINTR (      1,I       ,DUM    )
0028                IF (IACTIV(4)    .EQ.NZERO ) GO TO 40
0029                CALL STIFF
0030                CALL MOVEWD (A(N23),A(N22),NLOAD )
0031                CALL GLDISP
0032                CALL UENRGY (A(N22),A(N23),A(J23),A(M41),NEQUA )
0033                CALL PARTUD (A(J23))
0034             45 CONTINUE
0035                CALL STIFF
0036                IF (IACTIV(4)    .EQ.NONE  )
                   *CALL CBOUND (A(K23),A(N39),NEQUA ,NCBDN ,NBAND )
0037                CALL MOVEWD (A(N23),A(N22),NLOAD )
0038                CALL GLDISP
0039                IF (IACTIV(4)    .EQ.NZERO ) GO TO 45
0040                CALL UENRGY (A(N22),A(N23),A(J23),A(L41),NEQUA )
0041                CALL CALCKI (A(N17),A(M23),A(L23),A(J23),A(M41),A(L41),A(K41))
0042             45 CONTINUE
0043                CALL STRESS (A(N3) ,A(N4) ,A(N22),A(N4)),JMELMT,NEQUA )
0044                IF (IACTIV(4)    .EQ.NONE  )
                   *CALL KIPRNT (A(J23),A(K41))
0045                CALL ORDER  (SCALFT)
0046                CALL PRINTR (      2,IDUM  ,SCALFT)
0047                CALL LDCHCK (A(N28),A(N30),IDUM  ,IDUM  ,      2)
0048                KK     =0
0049                NN9    =N9     -NEQUA *2
0050                NN10   =N10    -NEQUA
0051                DO 25 J=1,NMDESV
0052                NN10   =NN10   +NEQUA
0053                CALL SEZERO (A(N15),NSTIF )
0054                CALL RCONST (A(NN10)      ,DUM    ,A(N15),A(N15),NEQUA ,KK     ,
                   *            0)
0055                IF (IACTIV(4)    .EQ.NONE  )
                   *CALL CBOUND (A(K23),A(N15),NEQUA ,NCBDN ,NBAND )
0056                CALL SEZERO (A(N41),NLOAD )
0057                NN9    =NN9    +NEQUA *2
0058                NN22   =N22    -NEQUA
0059                NN41   =N41    -NEQUA
0060                DO 30 K=1,NMLDCN
0061                NN22   =NN22   +NEQUA
0062                NN41   =NN41   +NEQUA
0063                CALL LDCHCK (IDUM  ,A(N30),K      ,KOK    ,      1)
0064                IF (KOK    .EQ.NZERO ) GO TO 30
0065                CALL MLTPLY (A(NN9),A(NN22)       ,A(N15),A(NN41)       ,NEQUA )
```

Fig.A2 Main Subroutine (2of3)

```
0066              CALL BACKS  (A(N8) ,A(NN41)       ,A(N29),NEQUA ,NBAND )
0067           30 CONTINUE
0068              CALL ORDENT (A(N4) ,A(N22),A(N23),A(J23),A(N24),A(N25),A(N26),
                *              A(N28),A(N40),A(N41),A(K41),A(J41),A(N42),NMDESV,
                *              NMELMT,NEQUA ,J      )
0069           25 CONTINUE
0070              CALL SEIZER (A(N29),NMDEAD)
0071              CALL ELIMNT (A(N29),A(N42),NMDESV,     1)
0072              CALL REDESN (SCALFT,I      )
0073              IF (KSTOP .EQ.NONE  ) GO TO 10
0074              CALL AREA   (A(N6) ,A(N11),A(N17),A(N20),DUM   ,DUM   ,NMELMT,
                *                 0)
0075              CALL PRINTR (     3,IDUM  ,DUM   )
0076           15 CONTINUE
0077              KLAST =1
0078              IPAREA=LPAREA
0079              IPDISP=LPDISP
0080              IPSTRS=LPSTRS
0081              IPCONS=LPCONS
0082              CALL PRINTR (     4,IDUM  ,DUM   )
0083              IF (IACTIV(4)   .EQ.NZERO ) GO TO 50
0084              CALL STIFF
0085              CALL MOVEWD (A(N23),A(N22),NLOAD )
0086              CALL GLDISP
0087              CALL UENRGY (A(N22),A(N23),A(J23),A(M41),NEQUA )
0088           50 CONTINUE
0089              CALL STIFF
0090              IF (IACTIV(4)   .EQ.NONE  )
                *CALL CBOUND (A(K23),A(N39),NEQUA ,NCBUN ,NBAND )
0091              CALL MOVEWD (A(N23),A(N22),NLOAD )
0092              CALL GLDISP
0093              IF (IACTIV(4)   .EQ.NZERO ) GO TO 55
0094              CALL UENRGY (A(N22),A(N23),A(J23),A(L41),NEQUA )
0095              CALL CALCKI (A(N17),A(M23),A(L23),A(J23),A(M41),A(L41),A(K41))
0096           55 CONTINUE
0097              CALL STRESS (A(N3) ,A(N4) ,A(N22),A(N40),NMELMT,NEQUA )
0098              IF (IACTIV(4)   .EQ.NONE  )
                *CALL KIPRNT (A(J23),A(K41))
0099              CALL ORDER  (SCALFT)
0100              CALL PRINTR (     2,IDUM  ,SCALFT)
0101              PRINT 2001
0102              PRINT 2001
0103              GO TO 5
0104           10 CONTINUE
0105              STOP
0106         2000 FORMAT (/////,19X,18H DESIGN CYCLE . = ,I5)
0107         2001 FORMAT (/////,13(10H**********))
0108         2002 FORMAT (1H1,/////,13(10H**********))
0109              END
```

Fig.A2 Main Suboutine (3of3)

Boundary conditions corresponding to suppressed nodes (to close the crack from A_2 to A_1) are imposed in CBOUND. Stress intensity factors are then calculated in CALCKI.

The third major function is the evaluation of the constraints, including the identification of near active constrains in ORDER. Gradients of the near active constraints are then obtained in GRDENT and dependent constraints are eliminated in ELIMNT.

The fourth major function is the iterative redesign. The calculation of the Lagrange multipliers and the design factors, the imposition of move limits, the trial resizing and the elimination of inactive constraints are accomplished in steering routine REDESN.

Input Data Preparation

Required input data cards are described fully in Appendix B. The following description is only for that portion of data which differs from the data required in ordinary finite element programs.

1. Design variable linking

Element sizing variables A_i (the areas of the truss elements and the thicknesses of the planar elements) are linked to design variables through the linking matrix a_{ij} so that

$$A_i = a_{ij} D_j \quad \begin{cases} i = 1,2,\ldots,N \\ j = 1,2,\ldots,m \end{cases} \tag{A1}$$

Generalized linking is provided; that is, different element types may be linked to the same design variable and elements may be linked to one or

more design variables. For each element it is necessary to specify the corresponding design variable and the value of the linking coefficient.

2. Constraint criticality buffer

A constraint is strictly critical if $g_k = 0.0$ or if $R_k = g_k + 1.0 = 1.0$. For numerical purposes, a constraint is assumed active and governing the redesign if

$$\text{FILTER} = 1.0 - \beta \leq R_k \leq 1.0 \tag{A2}$$

where β is the constraint criticality buffer and FILTER is the variable name of the quantity $1.0 - \beta$. Default values of FILTER (and the constraint criticality buffer β) are obtained by reading in a zero initial value.

3. Dependent constraint filter

The linear equations to solve for the Lagrange multipliers of active constraints, Eq. (18), are functions of the constraint gradients. The constraints for problems with symmetry linking are dependent, and therefore, so are the constraint gradients and the equations for the Lagrance multipliers. Dependent equations are eliminated by comparing constraint gradients term by term. Constraint gradients are assumed equal if the difference is less than ESIF where

$$\text{ESIF} = 10^{-\text{NSIF}} \tag{A3}$$

and NSIF is the expected accuracy of the computer in terms of the number of significant digits.

APPENDIX B

INPUT DATA DESCRIPTION

1) Control data, two cards.

Card 1: (20A4); heading

Card 2: (6I5)

columns 1-5; number of nodes.

columns 6-10; number of element types.

columns 11-15; number of elements.

columns 16-20; number of design variables.

columns 21-25; number of load conditions.

columns 26-30; number of design cycles.

2) Node point data input, one card per node (3E13.6, 3I5).

columns 1-13; x_1 coordinate

columns 14-26; x_2 coordinate.

columns 27-39; x_3 coordinate.

columns 40-44; code for x_1

columns 45-49; code for x_2 } = { 0, free.

columns 50-54; code for x_3 } { 1, constrained.

3) Element input.

one card per element type (4I5).

columns 1- 5; type number of element.

columns 6-10; number of elements of type.

columns 11-15; blank.

columns 16-20; blank.

element cards.

Card 1: (3E13.6, I5).

columns 1-13; elastic modulus.

columns 14-26; Poisson ratio.

columns 27-39; weight density.

columns 40-44; analysis option (1=plane stress, 2= plane strain).

one card per element (8I5)

columns 1- 5; node I.

columns 6-10; node J.

columns 11-15; node K.

columns 16-20; node L.

columns 21-25; node M.

columns 26-30; node N.

columns 31-35; node O.

columns 36-40; node P.

} nodes numbered counterclockwise from I - P

two cards per element

Card 1: (I5); design variable number.

Card 2: (E13.6); linking coefficient

4) Design variable input.

Card 1: (E13.6); default design variable.

Card 2: (2E16.6).

columns 1-13; default minimum value.

columns 14-26; default maximum value.

one card per design variable (3E13.6).

columns 1-13; design variable value.

columns 14-26; minimum value.

columns 27-39; maximum value.

5) Load data input.

one card per loaded node (2I5, 3E16.6).

columns 1- 5; node.

columns 6-10; load condition.

columns 11-23; x_1 component of load.

columns 24-26; x_2 component of load.

columns 37-49; x_3 component of load.

6) Constraint data input.

control card: (4I5); constraint activity.

columns 1- 5; stress activity

columns 6-10; displacement activity

columns 11-15; relative displacement activity

columns 16-20; fracture activity

$$= \begin{cases} 0, & \text{nonactive.} \\ 1, & \text{active.} \end{cases}$$

element cards (if IACTIV(1)=1).

Card 1: (2E13.6).

columns 1-13; default tensile yield.

columns 14-26; default compressive yield.

one card per element (2E13.6).

columns 1-13; tensile yield stress.

columns 14-26; compressive yield stress.

node cards (if IACTIV(2)=1).

Card 1: (2E13.6).

columns 1-13; default upper displacement limit.

columns 14-26; default lower displacement limit.

one card per node (2E13.6).

columns 1-13; upper displacement limit.

columns 14-26; lower displacement limit.

relative displacement cards (if IACTIV(3)=1).

Card 1: (E13.6); relative displacement limit

one card per constraint (6I5).

columns 1- 5; node A.

columns 6-10; node B.

columns 11-15; load condition.

columns 16-20; x_1 direction code

columns 21-25; x_2 direction code

columns 26-30; x_3 direction code

$$= \begin{cases} 0, & \text{relative displacement not active.} \\ 1, & \text{relative displacement active.} \end{cases}$$

fracture cards (if IACTIV(4)=1).

Card 1: (E13.6); intensity factor limit.

one card per load condition: (I5); load condition activity.

7) Crack data input (if IACTIV(4)=1).

Card 1: (3E13.6).

columns 1-13; crack area factor.

columns 14-26; crack length.

columns 27-39; crack extension.

one card per constrained crack node (5I5).

columns 1- 5; bounding element type.

columns 6-10; bounding element number.

columns 11-15; design variable number.

columns 16-20; initial crack front node.

columns 21-25; final crack front node.

8) Constraint elimination data input (3I5,3E13.6).

columns 1-5; number of constraint gradients calculated.

columns 6-10; blank.

columns 11-15; elimination option.

columns 16-28; ESIF.

columns 29-41; blank.

columns 42-54; FILTER.

9) Move limit data (2I5,2E13.6).

columns 1- 5; blank.

columns 6-10; fully stressing option.

columns 11-23; move limit Δ.

columns 24-36; fully stressing move limit I_j^*.

10) Print switch data input (5I5)

columns 1- 5; member area print switch.

columns 6-10; nodal displacement print switch.

columns 11-15; member stress print switch.

columns 16-20; constraint print switch.

columns 21-25; gradient print switch.

switch = 0, no print.

switch = 1, print.

APPENDIX C

FINITE ELEMENTS USED IN STRESS ANALYSIS

The stiffness relations for a linear elastic structure are

$$[K]\{u\} = \{F\} \tag{C1}$$

where the system stiffness matrix $[K]$ is obtained by direct addition of the element stiffness matrices $[K]_i$ with

$$[K]_i = \int_V [B]^T [E][B]dV \ . \tag{C2}$$

In Eq. (C2), $[B]$ is the linear strain displacement matrix for element i, $[E]$ is the matrix of elastic constants and V is the volume.

Brief derivations of the stiffness properties of the finite elements used in the present version of the design program are given below. The two-node truss element (TRUSS2) is a special case of the TRUSS3 element and the three-node triangle (CST) and the four-node quadrilateral (QUAD4) are special cases of the QUAD8 elements; therefore, the TRUSS3, the CST and the QUAD4 elements are not described separately. Further details of the stiffness calculation can be found in many texts, including Ref. 29.

Three-Node Three-Dimensional Truss (TRUSS3).

The three-node subparametric truss element is shown in Fig. C1. The coordinates x_1, x_2 and x_3 are system cartesian coordinates, S is a local coordinate along the truss varying from 0 to L (the truss length) and r is a natural corrdinate along the truss varying from -1 to +1.

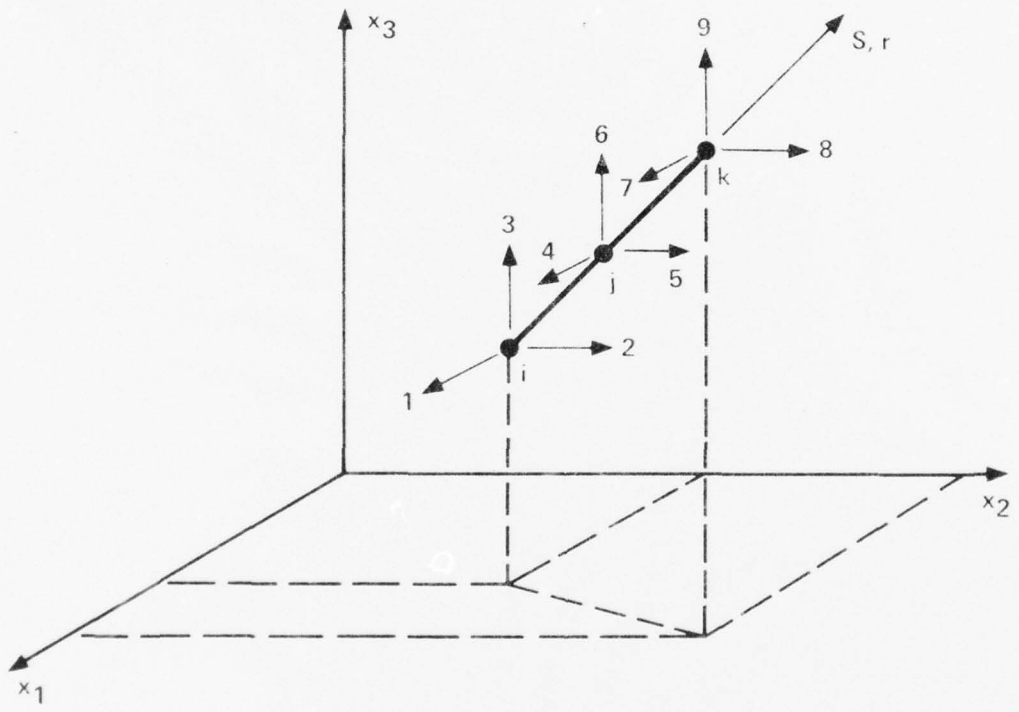

Fig. C1. Three Node Subparametric Truss Element

The displacement u along the truss is assumed quadratic in the natural corrdinate r, that is,

$$u = \left[\frac{1}{2}(1 - r) - \frac{1}{2}(1 - r^2)\right]u_i + \left[\frac{1}{2}(1 + r) - \frac{1}{2}(1 - r^2)\right]u_k + (1 - r^2)u_j \qquad (C3)$$

where u_i, u_j and u_k are the system displacements at nodes i, j and k, respectively. The system nodal displacements may be written in terms of the components along the system cartesian coordinates (u_{i1}, u_{i2}, u_{i3}, etc.) and the projected lengths of truss along the system coordinates (L_1, L_2 and L_3 where $L = \sqrt{L_1^2 + L_2^2 + L_3^2}$); that is,

$$\begin{aligned} u_i &= u_{i1}\frac{L_1}{L} + u_{i2}\frac{L_2}{L} + u_{i3}\frac{L_3}{L} \\ u_j &= u_{j1}\frac{L_1}{L} + u_{j2}\frac{L_2}{L} + u_{j3}\frac{L_3}{L} \\ u_k &= u_{k1}\frac{L_1}{L} + u_{k2}\frac{L_2}{L} + u_{k3}\frac{L_3}{L} \end{aligned} \qquad (C4)$$

The linear strain displacement relation is

$$\varepsilon = \frac{du}{dS} \qquad (C5)$$

The displacement is given in terms of the natural coordinate r and the strain displacement relation is in terms of the local coordinate S. Therefore, it is necessary to relate tne natural coordinate derivative and the local coordinate derivative to evaluate the strain. By the

chain rule

$$\frac{d}{dr} = \frac{dS}{dr}\frac{d}{dS} \equiv J\frac{d}{dS} \tag{C6}$$

where J is the Jacobian operator relating the natural and local derivatives.

The local position coordinate S is linear in terms of the natural coordinate r, that is,

$$S = \frac{L}{2}(1 + r) \tag{C7}$$

and $J = dS/dr = L/2$. The order of the position coordinate in r is less than the order of the displacement function; hence, the term subparametric [29].

The strain is

$$\varepsilon = \frac{du}{dS} = J^{-1}\frac{du}{dr}$$

$$= \frac{2}{L}\left[\left(-\frac{1}{2} + r\right)u_i + \left(\frac{1}{2} + r\right)u_k - 2r\,u_j\right] . \tag{C8}$$

Substituting for u_i, u_j and u_k from Eq. (C2) gives

$$\varepsilon = [B]\{u\} \tag{C9}$$

where

$$[B]^T = \frac{2}{L} \begin{Bmatrix} (-\frac{1}{2} + r)\frac{L_1}{L} \\ (-\frac{1}{2} + r)\frac{L_2}{L} \\ (-\frac{1}{2} + r)\frac{L_3}{L} \\ (\frac{1}{2} + r)\frac{L_1}{L} \\ (\frac{1}{2} + r)\frac{L_2}{L} \\ (\frac{1}{2} + r)\frac{L_3}{L} \\ -2r\frac{L_1}{L} \\ -2r\frac{L_2}{L} \\ -2r\frac{L_3}{L} \end{Bmatrix} \qquad \text{(C10)}$$

and

$$\{u\} = \begin{Bmatrix} u_{i1} \\ u_{i2} \\ u_{i3} \\ u_{k1} \\ u_{k2} \\ u_{k3} \\ u_{j1} \\ u_{j2} \\ u_{j3} \end{Bmatrix} . \qquad \text{(C11)}$$

The stiffness matrix is

$$[K]_i = \int_V [B]^T E[B]dV . \qquad \text{(C12)}$$

For constant truss area A,

$$[K]_i = A \int_S [B]^T E[B] ds$$

$$= A \int_{-1}^{1} [B]^T E[B] \frac{l}{2} dr \quad . \tag{C13}$$

Explicit integration is replaced by two-point Guass quadrature so that

$$[K]_i = \frac{AEL}{2} \sum_{j=1}^{2} W_j [B]_j^T [B]_j \tag{C14}$$

where W_j is the weighting function at integration point j and $[B]_j$ is the strain displacement matrix evaluated at integration point j.

Eight-Node Planar Quadrilateral (QUAD8).

The eight-node isoparametric planar element is shown in Fig. C2. The coordinates x_1 and x_2 are system cartesian coordinates and r and s are natural coordinates varying from -1 to +1.

The geometry of the element in the cartesian coordinates is "mapped" into a simple square in natural coordinates for ease in integration for the stiffness coefficients. The mapping or interpolating functions relate the cartesian and natural coordinate positions so that,

$$\left.\begin{aligned} x_1 &= \{\varphi_g\}^T \{\bar{x}_1\} \\ x_2 &= \{\varphi_g\}^T \{\bar{x}_2\} \end{aligned}\right\} \tag{C15}$$

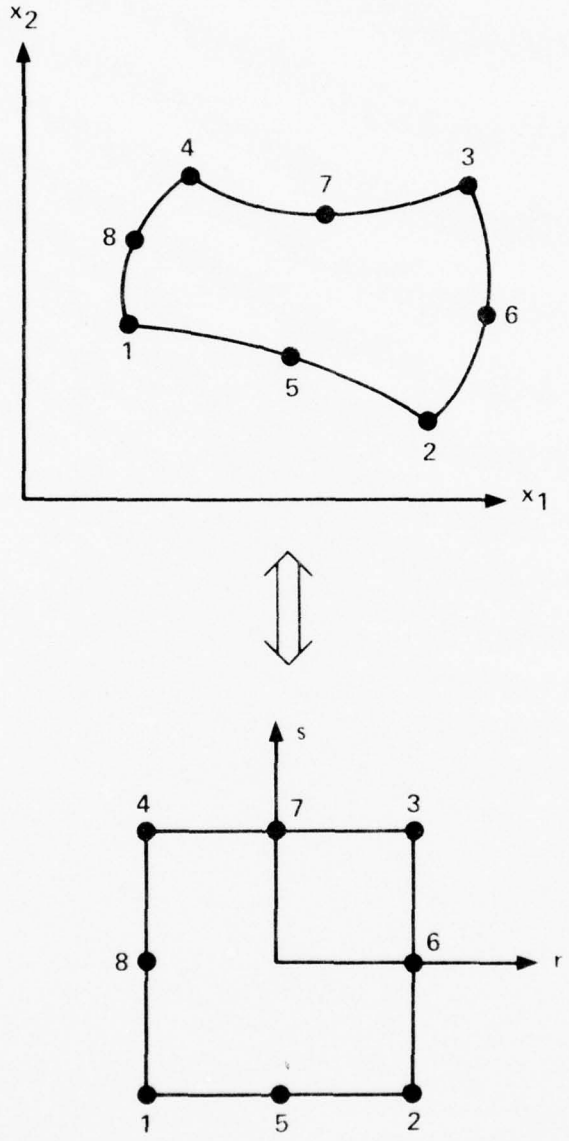

Fig. C2. Eight Node Planar Quadrilateral (QUAD-8) Isoparametric Finite Element

where

$$\{\varphi_g\}^T = \left\{ \begin{array}{l} \frac{1}{4}(1-r)(1-s) - \frac{1}{4}(1-r)(1-s^2) - \frac{1}{4}(1-r^2)(1-s) \\ \frac{1}{4}(1+r)(1-s) - \frac{1}{4}(1-r^2)(1-s) - \frac{1}{4}(1+r)(1-s^2) \\ \frac{1}{4}(1+r)(1+s) - \frac{1}{4}(1-r^2)(1+s) - \frac{1}{4}(1+r)(1-s^2) \\ \frac{1}{4}(1-r)(1+s) - \frac{1}{4}(1-r^2)(1+s) - \frac{1}{4}(1-r)(1-s^2) \\ \frac{1}{2}(1-r^2)(1-s) \\ \frac{1}{2}(1+r)(1-s^2) \\ \frac{1}{2}(1-r^2)(1+s) \\ \frac{1}{2}(1-r)(1-s^2) \end{array} \right\} \qquad (C16)$$

and $\{\bar{x}\}$ is the vector of nodal x_1 coordinate positions.

The displacements u_1 and u_2 along the x_1 and x_2 axis in terms of the natural coordinates are

$$\left\{ \begin{array}{c} u_1 \\ u_2 \end{array} \right\} = \left[\begin{array}{cc} \{\varphi\}^T & \{0\}^T \\ \{0\}^T & \{\varphi\}^T \end{array} \right] \left\{ \begin{array}{c} \{\bar{u}_1\} \\ \{\bar{u}_2\} \end{array} \right\} \qquad (C17)$$

where $\{\varphi\}$ are the interpolating or mapping functions and $\{\bar{u}_1\}$ and $\{\bar{u}_2\}$ are the vectors of the system nodal displacements along the x_1 and x_2 axes, respectively. The geometry and the deformation are the same order in the natural coordinates, that is $\{\varphi\} = \{\varphi_g\}$. Thus, the

QUAD8 is an isoparametric element [29].

The linear strain displacement relations are

$$\left.\begin{aligned} \varepsilon_{11} &= \frac{\partial u_1}{\partial x_1} \\ \varepsilon_{22} &= \frac{\partial u_2}{\partial x_2} \\ \varepsilon_{12} &= \frac{1}{2}\left(\frac{\partial u_1}{\partial x_2} + \frac{\partial u_2}{\partial x_1} \right) \end{aligned}\right\} \qquad (C18)$$

or

$$\{\varepsilon\} = \begin{Bmatrix} \varepsilon_{11} \\ \varepsilon_{22} \\ 2\varepsilon_{12} \end{Bmatrix} = \begin{bmatrix} \{\varphi\}^T_{,1} & \{0\}^T \\ \{0\}^T & \{\varphi\}^T_{,2} \\ \{\varphi\}^T_{,2} & \{\varphi\}^T_{,1} \end{bmatrix} \begin{Bmatrix} \{\bar{u}_1\} \\ \{\bar{u}_2\} \end{Bmatrix}$$

$$= [B]\{\bar{u}\} \quad . \qquad (C19)$$

It is necessary to relate the natural coordinate derivatives and the system coordinate derivatives to evaluate the strains. By the chain rule

$$\begin{Bmatrix} \frac{\partial}{\partial r} \\ \frac{\partial}{\partial s} \end{Bmatrix} = \begin{bmatrix} \frac{\partial x_1}{\partial r} & \frac{\partial x_2}{\partial r} \\ \frac{\partial x_1}{\partial s} & \frac{\partial x_2}{\partial s} \end{bmatrix} \begin{Bmatrix} \frac{\partial}{\partial x_1} \\ \frac{\partial}{\partial x_2} \end{Bmatrix}$$

$$= [J] \begin{Bmatrix} \frac{\partial}{\partial x_1} \\ \frac{\partial}{\partial x_2} \end{Bmatrix} \quad . \qquad (C20)$$

Therefore,

$$\begin{Bmatrix} \frac{\partial}{\partial x_1} \\ \\ \frac{\partial}{\partial x_2} \end{Bmatrix} = [J]^{-1} \begin{Bmatrix} \frac{\partial}{\partial r} \\ \\ \frac{\partial}{\partial s} \end{Bmatrix} . \qquad (C21)$$

Equation (C19) can be used to obtain the strain displacement matrix [B] in terms of the natural coordinates.

The stiffness matrix is

$$[K]_i = \int_V [B]^T [E][B] dV . \qquad (C22)$$

For constant thickness t,

$$[K]_i = t \int_A [B]^T [E][B] dA$$

$$= t \int_{-1}^{1} \int_{-1}^{1} [B]^T [E][B]|J| dr\, ds . \qquad (C23)$$

The explicit integration in the natural coordinates is replaced by Gauss quadrature so that

$$[K]_i = t \sum_{j=1}^{n} \sum_{i=1}^{n} w_j w_i [B(r_i, s_j)]^T [E][B(r_i, s_j)] \qquad (C24)$$

where w_i and w_j are the weighting functions, $[B(r_i, s_j)]$ is the strain displacement matrix evaluated at the integration point (r_i, s_j) and n is the integration order equal to 2, 3 or 4 (the larger values are necessary for accuracy with highly distorted elements).

APPENDIX D

EFFECT OF DESIGN VARIABLES ON LIFE OF STRUCTURES SUBJECTED TO CONSTANT AMPLITUDE CYCLIC LOADINGS

When linear elastic fracture mechanics is applicable the stable crack growth rate da/dN during constant amplitude cyclic loading (between σ_{max} and σ_{min}) can be expressed as

$$\frac{da}{dN} = \frac{da}{dN}(\Delta K, K_{mean}) \tag{D1}$$

where N is the number of cycles of loading, $\Delta K = K_{I_{max}} - K_{I_{min}}$, $K_{mean} = \frac{1}{2}(K_{I_{max}} + K_{I_{min}})$. The parameter $K_{I_{max}}$ is the stress intensity factor at $\sigma = \sigma_{max}$ and $K_{I_{min}}$ is the stress intensity factor at $\sigma = \sigma_{min}$ ($K_{I_{min}} = 0$ if $\sigma_{min} < 0$). Experimental results exhibit a linear relation between $\log (da/dN)$ and $\log (\Delta K)$ for constant values of mean stress (with significant deviation only near final failure) [30], that is,

$$\frac{da}{dN} = C_o(\Delta K)^n \tag{D2}$$

where C_o and n are empirical constants determined from the experimental results with n usually in the range $2.4 \leq n \leq 4.0$.

Solving Eq. (D2) for dN and integrating between the initial crack size a_i and the critical crack size a_c gives the number of cycles to failure N_ℓ (the life of the structure),

$$N_\ell = \frac{1}{C_o}\int_{a_i}^{a_c} \frac{da}{(\Delta K)^n} \, . \tag{D3}$$

The gradient of the life with respect to a design variable D_j is

$$\frac{\partial N_\ell}{\partial D_j} = \frac{1}{C_0} \left\{ \frac{1}{\Delta K^n(a_c)} \frac{\partial a_c}{\partial D_j} - n \int_{a_i}^{a_c} \frac{1}{(\Delta K)^{n+1}} \frac{\partial \Delta K}{\partial D_j} \, da \right\} . \qquad (D4)$$

The durability requirement in Ref. 20 states that $a_i = 0.125$ in. For fail-safe design of stiffened panels $a_c = a_t$, the threshold crack size. The stress intensity factor ΔK and the gradient $\partial \Delta K / \partial D_j$ can be calculated as discussed in Section IV. Then the integral equation for the life, Eq. (D3), and the integral expression for the life gradient, Eq. (D4), can be evaluated numerically. To complete the life gradient calculation it is necessary to evaluate $\partial a_c / \partial D_j$.

In the initial stages of crack growth, the crack length is small and the stiffener has little effect on the near crack tip stresses. Therefore, an approximate calculation for the critical crack gradient can be obtained using the analytic solution for a crack in an infinite sheet,

$$K_I = \sigma \sqrt{\pi a} \quad . \qquad (D5)$$

Equation (D5) is used only to estimate the gradient $\partial a_c / \partial D_j$ in Eq. (D4).

At the onset of fast fracture $a = a_c$ and $K_I = K_C$. Substituting $a = a_c$ and $K_I = K_C$ into Eq. (D5) and differentiating with respect to D_j gives

$$\frac{\partial K_C}{\partial D_j} = \sigma \frac{\partial}{\partial D_j} \left(\sqrt{\pi a_c} \right) + \left(\sqrt{\pi a_c} \right) \frac{\partial \sigma}{\partial D_j} \quad . \qquad (D6)$$

Solving for $\partial a_c / \partial D_j$ gives

$$\frac{\partial a_c}{\partial D_j} = -\frac{2a_c}{\sigma}\frac{\partial \sigma}{\partial D_j} + \frac{2\sqrt{\pi a_c}}{\pi\sigma}\frac{\partial K_c}{\partial D_j} \quad . \tag{D7}$$

For the example problem with design variables D_1, D_2 and D_3 (and assuming the crack in the stiffened panel acts as a crack in an infinite unstiffened sheet),

$$\sigma = \frac{q}{D_3} \tag{D8}$$

where q is the far field line load. Therefore,

$$\frac{\partial \sigma}{\partial D_j} = \begin{cases} 0 \quad , & j \neq 3 \\ -\sigma/D_j, & j = 3 \end{cases} \tag{D9}$$

so that

$$\frac{\partial a_c}{\partial D_j} = \delta_{j3}\,\frac{2a_c}{D_3} \tag{D10}$$

where δ_{j3} is the Kronecker delta. This result implies that K_c is constant over a sufficient range of D_3 (see Fig. 8).

Substituting Eq. (D10) into Eq. (D4), gives

$$\frac{\partial N_\ell}{\partial D_j} = \frac{1}{C_0}\left\{ \frac{1}{\Delta K^n(a_c)}\frac{2a_c}{D_3}\delta_{j3} - n\int_{a_i}^{a_c} \frac{1}{\Delta K^{n+1}}\frac{\partial \Delta K}{\partial D_j}\,da \right\} \quad . \tag{D11}$$

Numerical results for the stiffened panel with $D_1 = 0.5$ in.^{2}, $D_2 = 0.3$ in.^{2} and $D_3 = 0.07$ in. and $a = a_t = 5.0$ in. gives

$$\frac{\partial(K_I/K_C)}{\partial D_1} = -0.545$$

$$\frac{\partial(K_I/K_C)}{\partial D_2} = +0.00595 \cong 0.0 \qquad \text{(D12)}$$

$$\frac{\partial(K_I/K_C)}{\partial D_3} = -3.279$$

Since $\partial K_I/\partial D_j$ is proportional to $\partial\sigma/\partial D_j$ given a, these results show that for small cracks the skin has the greatest effect on the stress intensity factor, justifying the approximation of Eq. (D5) to estimate the critical crack gradient $\partial a_c/\partial D_j$. Also, it is obvious that

$$\frac{\partial N_\ell}{\partial D_j} \geq 0 \qquad j = 1,2,3 \qquad \text{(D13)}$$

showing, as expected, that a decrease in the design variables will decrease the life of the structure.

END 9-77
DDC